

Cost-Effective Climate Control System for Urban Slums in Bangladesh

Final Report

ME 450 Team 8: Rahul Saxena, Derek Tan, Maddy Trevisan, Mihir Upadhye, Betty Wan

Executive Summary

There is a need to improve the thermal comfort of urban slum residents located in Rayer Bazar, a region of Dhaka, the capital of Bangladesh. This need was first discovered by the University of Michigan's BLUElab student organization during a needs assessment trip to the area in August 2018. The group conducted extensive interviews during their trip in partnership with the Spreeha Foundation [1], a local non-governmental organization. This need was validated using climate data and literature quantifying human perceptions of thermal comfort. The three most important factors that influence human perception of thermal comfort are temperature, relative humidity, and indoor wind speed. For residents of Dhaka, these factors are severe between March and October and are summarized in Table 1 below. Additional contextual information from research is described in the Project Description section below (pg. 2).

Table 1: Summary of essential parameters that influence human perception of thermal comfort for Bangladesh.

| Temperature [°C] ^[2] | Relative Humidity [%] ^[3] | Indoor Wind Speed [m/s] ^[4] |
|---------------------------------|--------------------------------------|--|
| 22 – 35 | 55 - 80 | 0.05 – 0.48 |

The user requirements were largely determined from an interview with two members of the BLUElab team that conducted the needs assessment trip in Bangladesh. They described the current living conditions of residents of the Rayer Bazar slum, provided insight into their culture and daily routines, as well as shared important data collected during the interview. To satisfy the requirements, quantifiable engineering specifications were defined through the review of research papers, standards, and data sourced from governmental databases. The user requirements and engineering specifications, along with their respective sources, are summarized in Table 3 (pg. 6) below.

Individual brainstorming and functional decomposition techniques were used to generate concepts that would increase thermal comfort by decreasing temperature, decreasing humidity, and increasing air speed. These ideas were organized into a morph chart, shown in Table 4 (pg.13). The main concepts included direct evaporative cooling, ventilation via thermal chimney, a reflective tarp, thermoelectric cooling, and fan ventilation. Preliminary engineering analysis was conducted to allow for comparison of these concepts to a baseline solution in the Pugh Chart in Table 6 (pg.17). From this chart, the final selected concept to increase thermal comfort was thermoelectric cooling with fan ventilation.

The final design is presented on (pgs. 20-21), with a CAD model shown in Figures 22-23. A detailed engineering analysis justifying the final design is shown on (pgs. 22-34). Due to an inability to prototype and test because of COVID-19, engineering analysis using a Matlab model and CFD simulation was crucial in verifying the solution.

Figure 33 (pgs. 35-37) outlines a more detailed verification plan to assess the design's ability to meet user requirements and engineering specifications once it is safe to do so. A plan for user validation will be outlined and passed onto the BLUElab members for future testing of the prototype. The final estimated cost of this solution is \$43.34, which is within our target cost. This project will be passed onto BLUElab and discussed with Spreeha in hopes of successful implementation in the future.

Problem Description

In August 2018, members of BLUElab at the University of Michigan went on a needs-assessment trip to Dhaka, Bangladesh and identified the need to improve thermal comfort Rayer Bazar urban slums. Extensive interviews were conducted in the community with the support of their partner, the Spreeha Foundation, a non-governmental organization that provides services to improve quality of healthcare and education. Using climate data from published sources, it was discovered that residents of the urban slum in Rayer Bazar face discomfort in temperatures between 22°C to 35°C, relative humidity levels between 55% to 80% and indoor wind speeds between 0.05 m/s to 0.48 m/s. These values are summarized in Table 1 (pg. 1) above.

Additional contextual information was obtained from interviews and published literature. Houses in the urban slums are made from either corrugated tin sheets or cement, as shown in Figure 1 below. Interviews with the urban slum community revealed that houses made from tin sheets have higher temperature during the day and lower temperature during the night, compared to houses made from cement in similar conditions. This is because tin sheets are thinner ($t_{\text{tin}} = \sim 10^{-3} \text{ m}$ [5], $t_{\text{concrete}} = \sim 10^{-2} \text{ m}$ [5]) and have higher thermal conductivity compared to concrete walls ($K_{\text{tin}} = 67 \text{ W/mK}$ [6], $K_{\text{concrete}} = 1.0 \text{ W/mK}$ [7]), resulting in greater conductive heat transfer and therefore quicker realization of thermal equilibrium with ambient temperature. This comparison is reflected in Figure 1 below.



Figure 1: The slums are comprised of corrugated tin homes (left) and concrete homes (right). Most homes have small ceiling fans while some have windows [5].

Cooling is required during the day and night [8]. During the day, high ambient temperature causes high indoor temperature via radiative and convective heat transfer. During the night when it is time to sleep, the congregation of household members in the confined space generates heat, increasing indoor temperature and causing thermal discomfort.

In addition, these houses are often rented from landlords [8], implying that the solution space must not involve any structural modifications to the houses. These houses are mostly 3.0 m by 3.6 m [8], indicating a limit to the physical size of any potential solution. The absence of windows in most of these houses [8]

would limit potential solutions that involve airflow from ambient air. The current solution adopted by community members is the use of ceiling fans to increase indoor wind speed [8], as seen from Figure 1 (pg. 2).

It is also important to note that flooding can result in water levels up to 40 cm, especially during the monsoon season between June to October [4], as seen from Figure 2 below. To cope with the issue of household items being damaged from flooding, community members would usually elevate their items above ground, as seen from Figure 2 below. Flooding therefore limits the solution space to products that are either water-resistant or would avoid contact with the water during floods.

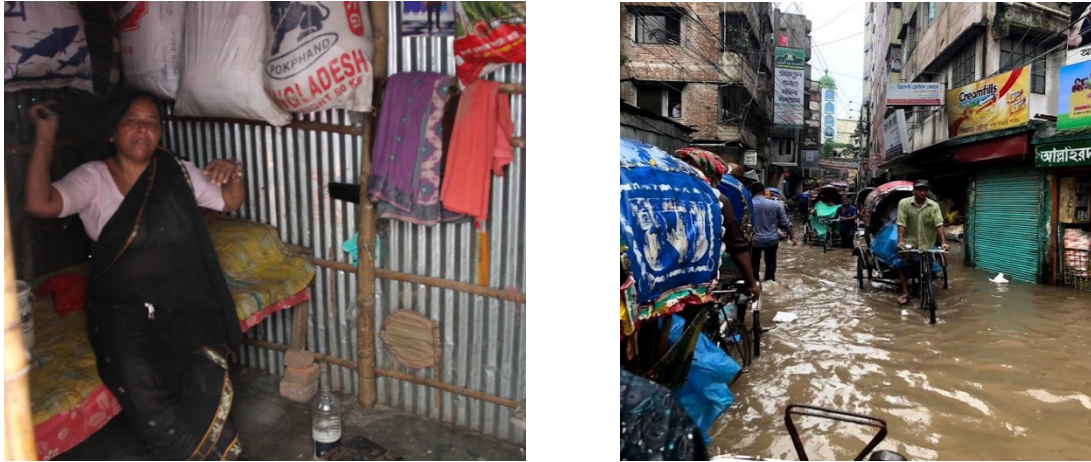


Figure 2: Flooding up to 40cm water level is common in Bangladesh (left) [5].

Information about residents' access to essential resources was also reported by a published source [9]. Approximately 20 to 40 families share access to water via tube-wells. While the families rely on the main electrical grids for electricity, they experience about two hours of electrical disturbance per day. Gas is supplied to shared kitchens about three to four times per day, lasting 30 to 50 minutes for each supply.



Figure 3: Slum residents would obtain drinking water from shared tube wells (left). Cooking is done in shared kitchens using limited gas supplied (right) [5].

With the support of Spreeha and BLUElab, the fabricated solution would be brought to Bangladesh for testing and validation as soon as it is possible and safe to do so.

Summary of Relevant Information Sources

Our relevant information sources can be broken down into three categories: stakeholders, subject matter experts, and published sources. Interviews with stakeholders supplied a contextual background of the urban slums and what the residents need. Meetings with subject matter experts provided an overview of existing solutions as well as methods for determining cost and usability in low-resource settings. Published sources were used to define testable specifications for user requirements formulated from gathered information. These sources and their respective levels of influence on the solution and potential impact by the solution are shown below in Table 2.

Table 2: A summary of the information sources used to develop the user requirements and engineering specifications. The influence of each source on the solution as well as the solution's impact on the source are also shown.

| Source | Impact | Influence |
|----------------------------------|--------|-----------|
| Urban Slum Residents | High | Low |
| Community Mobilizers | High | Medium |
| BLUElab Members | Medium | High |
| Local NGO - Spreeha | Medium | High |
| Subject Matter Experts | Low | High |
| Competing Devices & Benchmarking | Low | Medium |
| Patents | Low | Medium |
| Academic Literature | Low | High |

Stakeholders

Stakeholders include the urban slum residents, two members of the student organization BLUElab also working on this design problem, the Bangladeshi NGO Spreeha, and the community mobilizers working in the urban slums. Due to language barriers and the long distance between the University of Michigan and Rayer Bazar, the urban slum residents have yet to be contacted directly but are the end-users of any potential solution. To understand more about their needs, lifestyles, and available resources, an interview was conducted with Abrar Iqbal and Kiersten White, two BLUElab members who visited the region in August 2019. The information gathered from this interview was key in identifying the design constraints set by resource limitations of the slum residents and other environmental factors. However, it was understood that this information was not from the residents themselves, so Spreeha was contacted to help verify resource constraints. To do this, Spreeha agreed to reach out to community mobilizers, former slum residents who act as the bridge between the community and the NGO. This indirect method of communication has caused a delay in receiving responses. Due to these communication barriers, the urban slum residents, the main end-users of a solution, have low direct influence on the solution specifications. The BLUElab members have high influence on the design process, as they are the source of most of the contextual information and design constraints. Spreeha and the community mobilizers have medium-to-high influence on the design process, as verification of resource limitations could affect the design space. As for the impact that a solution will have on these information sources, the urban slum residents will be impacted the most. The solution will have medium impact on the BLUElab members, Spreeha, and the community mobilizers due to their investment in the design and implementation process.

Subject Matter Experts

Subject matter experts include Professor Massoud Kaviani, Professor Kathleen Sienko, Caroline Soyars, Grace Burleson, and Joanna Thielen. Professor Kaviani, an expert in heat transfer, provided us with

various existing climate control solutions to consider for benchmarking. Professor Sienko, an expert in designing for low-resource settings, provided us with insights regarding approaching cost and usability metrics and their role in the design process. She directed us to two members of the Center for Socially-Engaged Design (CSED), Caroline Soyars and Grace Burleson, both of which have expertise in medical device implementation in low-resource settings. These two helped further with cost and usability and will continue to be an information source as the project progresses. In tandem with these meetings, Joanna Thielen was contacted to aid in navigating through published sources using the University of Michigan's library web portal. She shortlisted databases that would be the most useful for the design problem and provided search methodology that allowed for concise and specific filtration of published sources. These experts all have high influence on the solution, as their guidance has affected the view of the design problem and access to further information gathering. Since these sources will not be directly affected by a potential solution, the impact of the design process on them is minimal.

Published Sources

Published sources include academic literature, standards, and patents. Academic literature provided a peer-reviewed metric for thermal comfort, as well as temperature and humidity data for the region of interest. Multiple papers from various journals were considered when formulating the engineering specifications to ensure maximal coverage of environmental conditions experienced by urban slum residents. With the guidance received from Professor Sienko and Joanna Thielen, standards for usability were found for use in defining engineering specifications. Standards for durability and safety were found via ASHRAE and IEC standards. Patents were reviewed for benchmarking in the concept selection phase. All of these sources will not be impacted by a solution, but their role in defining engineering specifications highly influences the solution.

Information Gaps

Information that still needs to be found includes verification of resource limitations in Rayer Bazar, direct perspectives of urban slum residents, patent benchmarking of climate control systems in low-resource settings, and models to determine the potential solution's cost. The verification of resource limitations will come from the community mobilizers via Spreeha. Efforts to directly contact the urban slum residents are underway. Meanwhile, indirect communication via the community mobilizers is currently the best method to contact the end-users. Patent benchmarking will be done through database search and will aid in concept generation as well as increase the general intuition about possible solution performance. Cost determination of the product will continue to take shape as initial designs are selected for in-depth consideration – Caroline Soyars and Grace Burleson will be contacted as the design process becomes more solution-specific.

User Requirements and Engineering Specifications

The user requirements were largely determined from an interview with two members from BLUElab who attended the needs assessment trip in Bangladesh. The BLUElab members were able to provide details about the current living conditions of the people in Rayer Bazar, insights into their culture and daily routines, as well as supply data regarding household incomes. Since DR1, information gathered from Spreeha has allowed us to solidify and modify some of the requirements and engineering specs, which are discussed in more detail below. Other information sources used to develop requirements include subject matter experts, academic literature, current HVAC standards set by ASHRAE, Bangladesh weather and climate data, and existing solutions. Engineering specifications necessary to satisfy these requirements were then defined, all of which are quantifiable, testable and data driven. These specifications were set using the information sources as references for researching existing solutions, benchmarking, and identifying design constraints. Table 3 (pg. 6) shows the ranked user requirements, their corresponding engineering specifications, and the sources used to define each specification.

Table 3: A summary of the user requirements and engineering specifications that were developed for the potential solution.

| User Requirement | Engineering Specification | Certain | Neutral | Not Certain |
|--|--|---------|---------|-------------|
| 1. Safe | 0 potential electrical, fire, or chemical hazards in accordance with ISO 5149-1 [8] [10] [11] 0 sharp features and exposed moving parts [11] If system requires mounting, the mounting mechanism withstands the weight of the system by a safety factor of ≥ 2 [11] | | | |
| 2. Affordable | Target price (without subsidies): \$25 - \$50 (2000 - 4000 Tk) [8] | | | |
| 3. Adequate Cooling Ability | Cool the air near residents to [$\leq 30^{\circ}\text{C}$ at 0.15 – 0.30 m/s air speed] OR to [$\leq 32^{\circ}\text{C}$ at 2.2m/s air speed], $\leq 85\%$ relative humidity [4] | | | |
| 4. Compatible with Various Types of Houses | Meets all requirements in both sheet metal and concrete house types [8] | | | |
| 5. Easily Operated | Usability Metric: # of steps required to operate: ≥ 2 (Ex: on-off, or add water) [8] [12] Likert scale average rating of ≥ 3 for perceived usability (1=not usable, 4=very usable) [13] | | | |
| 6. Easily Installed | # of steps required: ≤ 3 [12] # of tools required: ≤ 1 (provided) [12] No technical ability required for installation [12] No physical or chemical alteration of existing structure [8] If mounting overhead: system mass $\leq 5 \text{ kg}$ [14] | | | |
| 7. Durable (Resilient to Environmental Factors) | Maximum Operating Temperature: $\geq 45^{\circ}\text{C}$ [15] Maximum Operating Relative Humidity: $\geq 90\%$ [16] System is IP52 rated - its function is not affected by dust and water dripping at up to a 15° angle from vertical (IEC 61032:1997) [17] Operate in a room with $\geq 40\text{cm}$ of water [18] | | | |
| 8. Reliable | If using electricity: successful operation ≥ 22 hours per day for a lifetime ≥ 2 years [8] | | | |
| 9. Easily Repaired or Replaced | Product has modular parts so that if any part fails, it can be replaced without replacing the whole system [19] [20] | | | |
| 10. Sustainable | No single-use plastics (Single-use plastics are banned in Bangladesh) [21] | | | |

The engineering requirements and their corresponding specifications from Table 3 (pg. 6) are described in more detail below, along with their rationale. Note that the user requirements are presented in order of importance.

Safe

The most important requirement for the climate control system is safety. Ensuring that the system is safe is the first step to building trust with the local community. Therefore, its design must avoid any potential electrical, fire, or chemical hazards. Additionally, to prevent physical harm, the system must not have any sharp features or exposed moving parts. If the system requires mounting, the mounting solution must withstand the weight of the system by at least a safety factor of 2. These requirements were derived from academic literature [10] and existing standards for heating and refrigeration equipment [11].

Affordable

It is important that the climate control system is accessible to as many urban slum residents as possible, so the system's cost must be affordable. Financial information of residents was collected by BLUElab members that travelled to Bangladesh last summer. From the interview with members of the BLUElab team [8], it was gathered that residents do not save much money or use banks. Residents tend to work and earn money as needed to pay for their food, rent, and other expenses. However, it should be noted that due to the personal nature of earnings and savings, the information provided may not be accurate. Additionally, since the BLUElab team only visited a few locations in the area, the information acquired may not be reflective of the entire population. Due to this uncertainty, Professor Sienko, an expert in design for low-resource settings, was consulted to help set a target cost. It was determined that the target cost of the device would be an estimate that will likely change throughout the design process as new information is discovered. The preliminary target cost of the device is less than 2000Tk, or roughly \$24. This cost was set by determining the local price [23] of compact, 0.61m-diameter fans that are found in most homes [8]. Since landlords or residents have purchased these fans, it provides a benchmark for how much money they are willing to spend to be more comfortable. Thus, it is reasonable to assume that the residents would be willing to spend a similar amount of money on this climate control system. After a meeting with Spreeha representatives, who are in contact with community mobilizers, it was discovered that there are some competing cooling solutions that cost a minimum of 5500Tk. This price is too high for a majority of the residents to afford. Thus, this solidifies the cost requirement of being 2000-4000Tk.

Adequate Cooling Ability

It is necessary that the climate control system cools residents to a level of comfort. Through academic literature it was found that human comfort depends on several parameters - the most important are temperature, humidity, and average wind speed. Additionally, the comfortable combination of parameters for those living in modern climate-controlled spaces are different from those living in spaces without any climate control. A study conducted in Bangladesh [4] showed that a desired comfort level is reached when the temperature and relative humidity are less than or equal to 30°C and 85%, with an average air velocity between 0.15 and 0.30 m/s, or less than or equal to 32°C with an average air speed of 2.2 m/s. It should be noted that these cooling specifications are based on explicit research regarding perceived cooling comfort in humid climates. The residents themselves are unable to provide exact numbers regarding ideal temperature and humidity reduction, which is why this specification remains "neutral."

Compatible with Various Types of Houses

It is important that the climate control system can operate successfully for as many urban slum residents as possible, so the system must function in the various types of houses in the area. The two most common types of houses are those made with concrete and those made with sheet metal panels [8]. Thus, the system must meet all requirements and specifications in both house types.

Easily Operated

It is crucial that climate control system is easily operated to have a low barrier to implementation. The solution must be intuitive to use and be well perceived by the community so that it is easily adopted. It must have a maximum of 2 steps required to operate and maintain per day, based on literature of existing standards [12]. The perceived usability will be evaluated using a Likert scale, with 1 meaning “not usable” and 4 meaning “very usable”. The solution must have an average score of 3 or higher to validate this requirement [13].

Easily Installed

The climate control system must be easily installed so that it can be used right away. To meet this requirement, the solution must be installed in a maximum of 3 steps, with only 1 required tool [12]. This specification will depend on the type of solution chosen. If wall mounting is involved, it is crucial that it does not impede on the other side of the wall, as residents of different families share the same walls. There should be no technical ability required to install the system, which also should not alter the physical or chemical properties of the existing house structure [8]. Finally, if the climate control system requires mounting, the system must weigh 5 kg or less to avoid causing physical strain [14].

Durable

It is important that the climate control system is durable as well as resilient to environmental factors. This means it must operate effectively in conditions of up to 45°C and 90% relative humidity [15][16]. Furthermore, this system should satisfy an IP52 rating, meaning its function is not affected by dust or water penetration at an angle of up to 15° from vertical [17]. Finally, it cannot be ruined by flooding during the monsoon season, and therefore needs to operate in at least 40 cm of flood water [18].

Reliable

If the climate control system requires a power source, it must be able to function at all times when there is access to electricity. This can be up to 22 hours a day. If the solution is passive, then it must operate 24 hours a day, since residents will be in and out of their homes throughout the day and will need cooling for comfort at night. It has been confirmed by Spreeha that there is indeed access to electricity 24/7, with the exception of occasional power outages during the summer. Therefore, the solution can rely on electricity. Perhaps the most crucial aspect of reliability is that the device is capable of running at any time of day, so that it is usable when the residents need it the most, such as right before bed. The expected lifetime of this device is 2 years [8][24]

Easily Repaired or Replaced

The climate control system should also be easily repaired or replaced. Through academic literature [19] [20], it was found that modular designs are best to use, as they allow for easy repairs without the need to replace the whole system.

Sustainable

Sustainability is also desired, considering the already-dire living conditions of the urban slum residents. The system must not contain or implement single-use plastics, as they are banned in Bangladesh [21].

Concept Generation

We began the concept generation process with a functional decomposition and individual brainstorming of cooling methods. The brainstorming was done separately to promote variety of ideas. After brainstorming, we collaborated and sorted our concepts based on which functions they directly applied to. These concepts were then placed on a morphological chart to aide in concept selection.

Functional Decomposition

After brainstorming cooling methods, we performed a functional decomposition of the concepts. The sub-functions identified include reducing temperature, reducing humidity, and increasing indoor air speed. Concepts to achieve these sub-functions are discussed in more detail below.

Solution Concepts to Reduce Temperature

The first solution concept identified to reduce temperature is a Vapor Compression Refrigeration Cycle (VCRC) system. Illustrated in Figure 4, this system leverages phase changes of a working fluid to transfer heat from one control volume to another. The cycle utilizes thermodynamic systems to move the working fluid, and includes a compressor, evaporator, throttle, and condenser to do so.

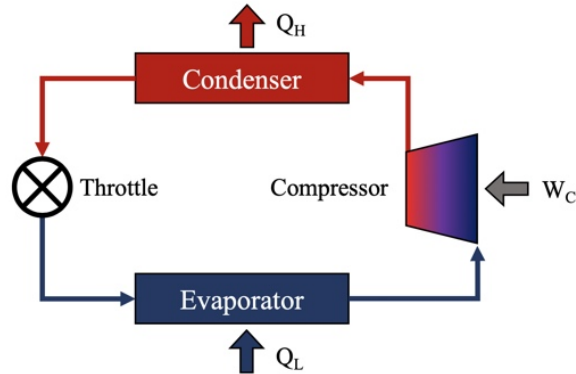


Figure 4: VCRC System

Similarly, an Absorption Refrigeration Cycle (ARC) also transfers heat from one control volume to another with a working fluid. However, instead of having a compressor, an ARC leverages the solubility of the working fluid in another fluid as well as thermal energy from the sun and solar collector. This is shown in Figure 5 below.

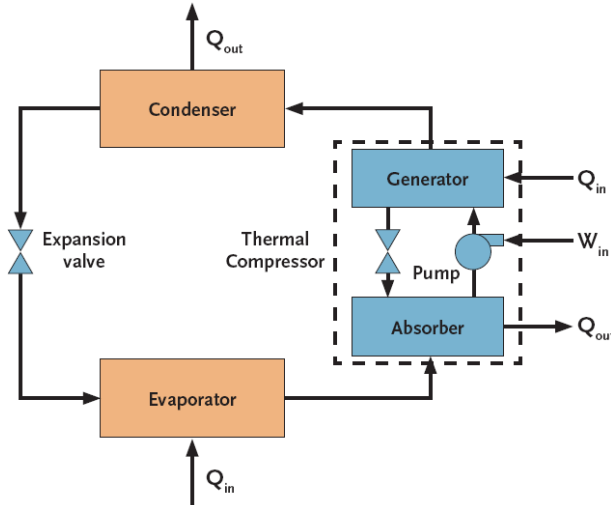


Figure 5: Absorption Refrigeration Cycle [25]

Evaporative cooling also reduces temperature by pulling heat out of the environment to vaporize water. This can be achieved directly to an air flow, in which case humidity increases. Indirect evaporative cooling cools air that is separated by a chamber, which does not cause an increase in humidity, but as a result is less efficient. Direct evaporative cooling is shown in Figure 6 below.

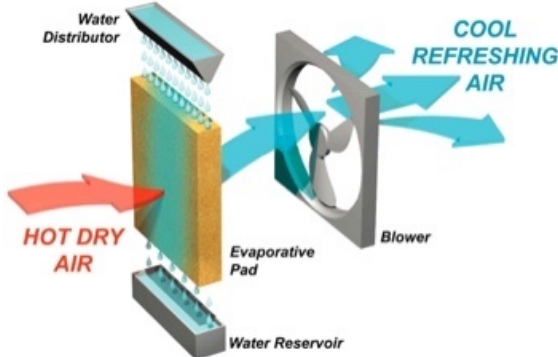


Figure 6: Evaporative Cooling System [26]

A reflective tarp or coating can also decrease temperature by reflecting solar radiation to prevent heat from penetrating the layer. This decreases the heat flux into the home. Such a tarp is shown in Figure 7 below.



Figure 7: Reflective Tarp [27]

Finally, thermoelectric cooling transfers heat using semiconductors, which is shown in Figure 8 below.

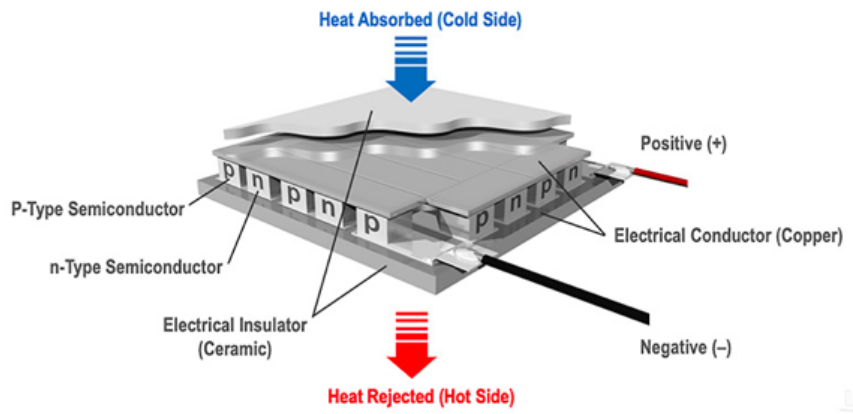


Figure 8: Thermoelectric Cooler [28]

Solution Concepts to Reduce Humidity

A simple way to reduce humidity is the use of a desiccant, which is a chemical compound such as Drierite or silica gel that absorbs a fixed amount of moisture (see Figure 9 below).



Figure 9: Common desiccants (Drierite left, silica gel packets right) [29, 30]

A refrigerant-based dehumidification system can also be used to decrease humidity, as illustrated in Figure 10 below. This system is relatively complex and costly to manufacture, however.

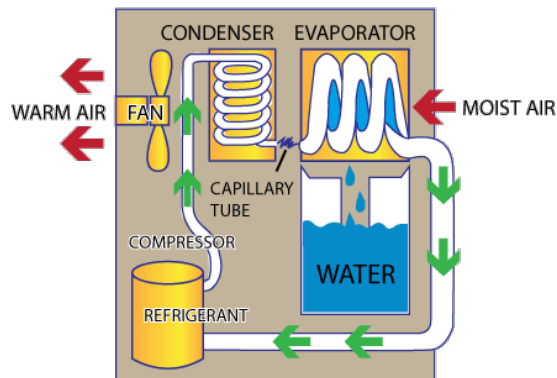


Figure 10: Refrigerant based dehumidification [31]

Finally, a passive way to decrease humidity is by introducing plants to the environment, since plants absorb water vapor in the air (Figure 11). This may not be a feasible solution, however, due to concerns of unwanted environmental impact, unnecessary maintenance, and possibility of overgrowth.



Figure 11: Plant to absorb moisture [32]

Solution Concepts to Increase Air Speed

The first concept identified to increase indoor air speed is a thermal chimney. This device creates natural ventilation due to an air density gradient created by a temperature differential, as illustrated in Figure 12 below.

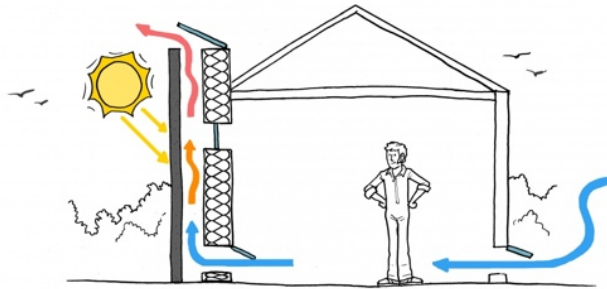


Figure 12: Thermal chimney concept sketch [33]

Another way to increase air speed is by modifying the current fans already in use in the residents' homes. This could involve mounting some sort of damp filter to cool the air circulating by evaporative cooling, as sketched in Figure 13 below.

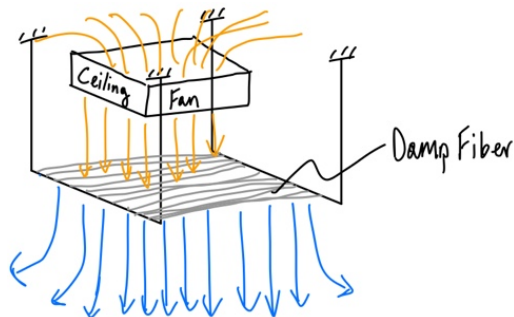


Figure 13: A sketch of a modification to existing fans used by residents

Finally, the most obvious way to increase air speed is by adding a standalone, portable, or hand-held fan to the living space. A standalone wall-mounted fan is shown in Figure 14 below.



Figure 14: Standalone fan [34]

Morphological Chart

The Morphological chart shown in Table 4 below organizes all the concepts discussed into their sub functions.

Table 4: Morphological Chart of solution concepts to improve thermal comfort.

| Item | Reduce Temperature | Reduce Humidity | Increase Indoor Air Speed |
|------|---|---|---------------------------|
| 1 | Vapor Compression Refrigeration Cycle | Desiccant Dehumidifiers (Solid / Liquid) | Thermal Chimney |
| 2 | Absorption Refrigeration Cycle | Refrigerant-Based Dehumidification | Current Fan Modification |
| 3 | Evaporative Cooling (Direct or Indirect) | Indoor Plants | Standalone Fan |
| 4 | High Reflectivity + Low Absorptivity Tarps or Coatings | | Portable Handheld Fan |
| 5 | Thermoelectric Cooling | | |

The morphological chart aided in the concept organization process and proved that a final solution must be a combination of concepts to satisfy the adequate cooling ability requirement.

Concept Evaluation and Selection

To properly assess these solutions, more information regarding their feasibility and performance was required. Preliminary engineering analysis was conducted for evaporative cooling, the thermal chimney, the reflective tarp, thermoelectric cooling, and fan ventilation concepts. These concepts were chosen for further analysis because it was unclear whether they would adequately cool the system. We did not conduct an in-depth engineering analysis for the VCRC system because there is an abundance of published data about this system that indicates that it cools adequately even in hot, humid climates. Following this analysis, the solutions were compared to each other using a Pugh Chart. Since empirical testing was not feasible due to COVID-19, the final solution selection was heavily based on the results from these preliminary calculations. The final concept selected was thermoelectric cooling, supplemented with fan ventilation.

Evaporative Cooling Analysis

The outlet temperature and relative humidity of air flowing through a channel with a wet surface were calculated given specific inlet air conditions using two governing equations. First, the principle of energy conservation balances convective heat transfer and mass transfer along with any external heat, shown in Equation 1. Second, the Clausius-Clapeyron relation relates pressure to temperature using the ideal gas law, shown in Equation 2. Both equations were solved simultaneously to obtain the density of water vapor in air at the wet surface of the channel, $(\rho_{f,w})_s$, and the surface temperature of the wet surface, T_s .

$$Q_s + \frac{T_s - T_{f,\infty}}{\langle R_{ku} \rangle_L} = -\frac{(\rho_{f,w}/\rho_f)_s - (\rho_{f,w}/\rho_f)_{\infty}}{\langle R_{ku} \rangle_L c_{p,f} \text{Le}^{-2/3}} \Delta h_{lg} \quad (1) [36]$$

$$p_{f,w} = (p_{f,w})_o \exp \left[-\frac{M_w \Delta h_{lg}}{R_g} \left(\frac{1}{T_s} - \frac{1}{T_{lg,o}} \right) \right] \quad (2) [36]$$

The heat absorbed from the air flow due to evaporative cooling, Q_{ku} , and the mass flow of water from the wet surface to the air, \dot{M}_{lg} were then calculated using Equations 3 and 4 relatively. In this application, Equation 4 is expressed in this form because Q_s from Equation 1 is 0.

$$Q_{ku} = \frac{T_s - T_\infty}{R_{ku}} \quad (3) [36]$$

$$\dot{M}_{lg} = \frac{(\rho_{f,w}/\rho_f)_s - (\rho_{f,w}/\rho_f)_\infty}{\langle R_{Du} \rangle_L} \quad (4) [36]$$

Finally, the calculated parameters were used in Equations 5 and 6 respectively to derive the outlet air temperature and relative humidity.

$$T_{out} = T_{in} + \frac{Q}{\dot{m}C_p} \quad (5) [36]$$

$$(\rho_{f,w})_o = (\rho_{f,w})_i + \frac{\dot{M}_{lg}}{U_f A} \quad (6) [36]$$

The density of water was converted to relative humidity using Tetens' approximation [37] and the ideal gas law. Equation 7 below provides the conversion.

$$RH = \frac{\rho_{f,w}RT(1000)}{M [0.61078 \exp\left(\frac{17.27T}{T+237.3}\right)]} \quad (7) [36]$$

It is essential to acknowledge that parameters such as surface temperature and water vapor density in air change as a function of distance travelled in the wet channel. A Matlab model was written to recalculate these parameters for increments of distance travelled by the air in the wet channel. Figures 15 and 16 show the air temperature and relative humidity with as a function of distance for a tube length of 0.3 m and 0.5 m respectively.

$T_{in} = 308 \text{ K}$, $RH_{in} = 70 \%$, $U = 5 \text{ m/s}$, Length Tube = 0.3 m, Surface Area Multiplier = 1.3
(Number of Iterations = 100)

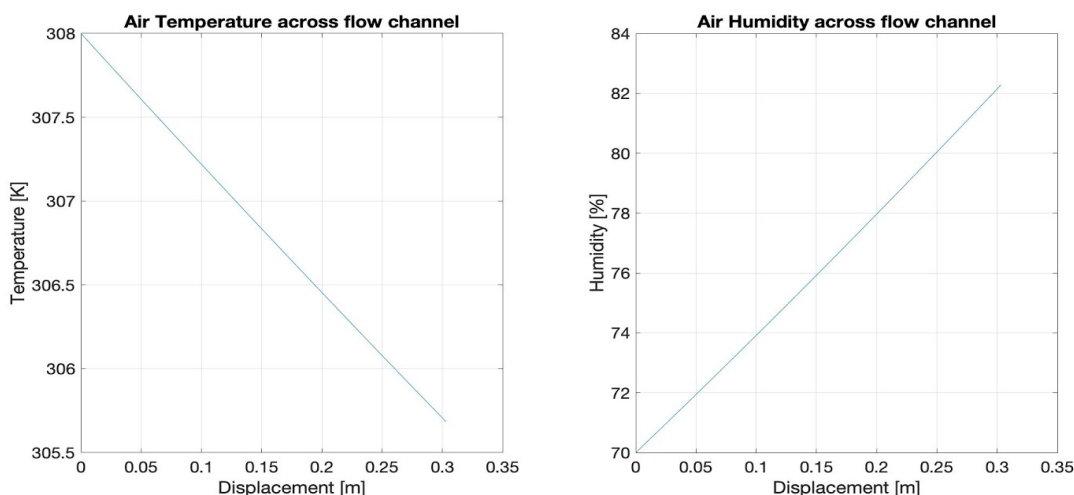


Figure 15: Air temperature and humidity through a tube 0.3m long.

$T_{in} = 308 \text{ K}$, $RH_{in} = 70 \%$, $U = 5 \text{ m/s}$, Length Tube = 0.5 m, Surface Area Multiplier = 1.3
(Number of Iterations = 100)

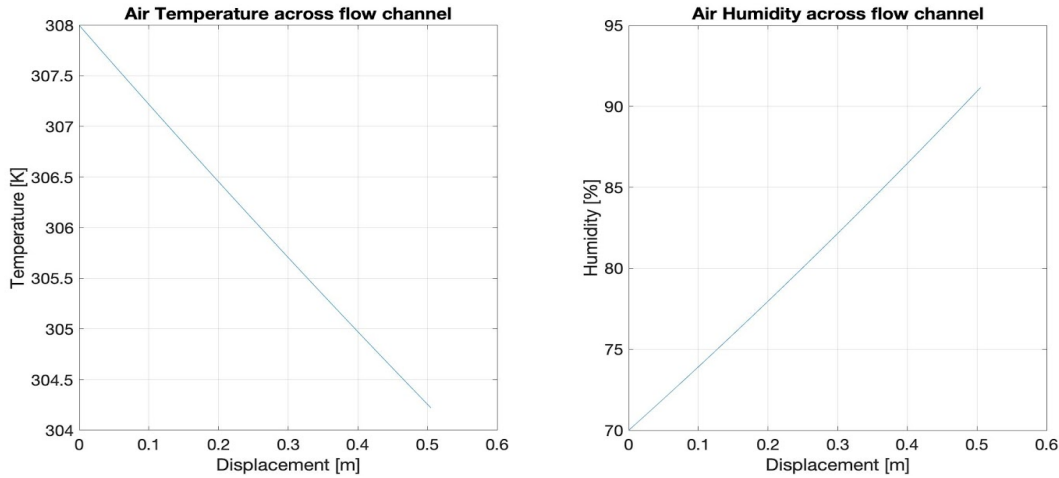


Figure 16: Air temperature and humidity through a tube 0.5 m long.

From Figure 15, it is observed that the system is cooled by 2.25°C while relative humidity increases by 12%. From Figure 16, it is observed that the system is cooled by 3.75 degrees while the relative humidity increases by 22 %.

Thermal Chimney Analysis

The extended Bernoulli equation (Equation 8) and principle of mass conservation (Equation 9) were employed to better understand how a thermal chimney can ventilate a house in Bangladesh. The equations are presented below:

$$\frac{p_1}{\gamma} + \alpha_1 \frac{V_1^2}{2g} + z_1 = \frac{p_2}{\gamma} + \alpha_2 \frac{V_2^2}{2g} + z_2 + h_L \quad (8) [35]$$

$$\rho_1 A_1 V_1 = \rho_2 A_2 V_2 \quad (9) [35]$$

where p_1 and p_2 are the inlet and outlet pressures, V_1 and V_2 are the inlet and outlet air velocities, z_1 and z_2 are the heights of the inlet and outlet, ρ_1 and ρ_2 are the densities of the inlet and outlet fluid, A_1 and A_2 are the inlet and outlet cross-sectional areas, γ is the specific weight at the inlet and outlet, and h_L is the head loss due to friction in the flow. α_1 and α_2 are the kinetic energy coefficients and are both equal to one, assuming uniform velocity profiles. For this analysis, a thermal chimney with a diameter of 0.3 m and height of 1.5 m was chosen, as these dimensions allow for a retrofit approach to the urban slum households. Plausible temperature differences were prescribed to calculate the inlet and outlet air densities. The flow was assumed to have constant pressure and constant cross-sectional area. The head loss term was calculated using a friction factor term found via the Reynolds number and a trade diagram [35]. Table 5 shows the resultant inlet air velocities caused by rising air due to various prescribed temperature differences.

Table 5: Various temperature differences and their resultant inlet air speeds.

| $\Delta T (\text{ }^\circ\text{C})$ | Inlet Air Speed (m/s) |
|-------------------------------------|-----------------------|
| 0.5 | 0.65 |
| 1.0 | 0.92 |
| 1.5 | 1.13 |
| 2.0 | 1.30 |

It was found that the thermal chimney can provide reasonable ventilation for expected temperature differences. However, it must be noted that thermal chimneys can only aid in ventilation during the day, and this is a major downside to this concept.

Reflective Tarp and Coating Analysis

A thermal circuit diagram, shown in Figure 17 below, was created to model the thermal heat flux and to assess the effectiveness of the proposed reflective tarp solution. The current tin roof consists of tin sheet and a thin layer of bamboo fencing placed underneath. The proposed solution involves adding highly reflective coating (e.g., white paint) and a thick insulation layer (e.g., polyurethane) on top of the tin sheet.

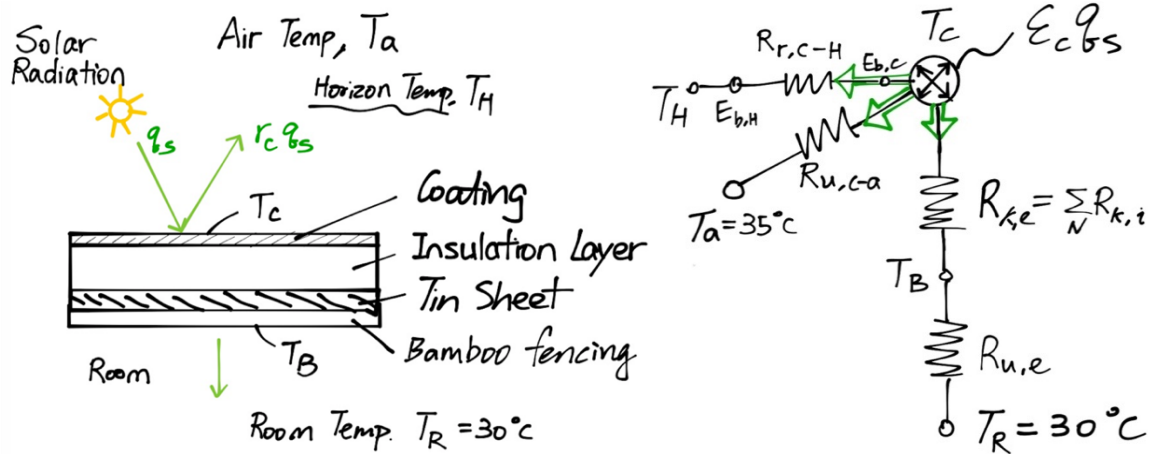


Figure 17: Thermal model of solar radiation on tin roof (left), and the thermal circuit diagram (right).

Solar radiation first contacts the coating, some radiation is reflected, some are radiated and convected to the atmosphere, and some are absorbed into the roof by conduction heat transfer through a series of roofing materials, eventually convected to the room.

With a model using white coating and 5cm-thick polyurethane as insulation layer, the total heat flux entering the room is estimated to decrease by 79%, comparing to a roof without additional coating and insulation. Thus, we see the reflective tarp as a promising solution at reducing heat flux and indoor room temperature.

Fan Ventilation Analysis

Based on academic literature, fan ventilation is most effective in providing cooling comfort when the airflow is directed at the core of the body, rather than upper or lower extremities. Furthermore, empirical testing has shown that increasing airflow speed by just 0.23 m/s can offset a 1°C increase in temperature to maintain a constant thermal comfort level [38]. An airspeed of 2.2 m/s was identified as the optimal speed to maintain a neutral thermal comfort level in hot, humid conditions [39]. The Center for the Built Environment developed a thermal comfort tool that approximates thermal comfort ranges based off of various inputs including ambient temperature, airspeed, relative humidity, metabolic rate, and clothing level. Using the tool, it was found that decreasing the air temperature by only 3°C while keeping all other inputs the same yields in an operating point near the edge of the thermal comfort zone. Therefore, a solution that can decrease the air temperature combined with a fan that can increase airflow would cool to enough to achieve thermal comfort conditions [40]. This result is shown in Figure 18 below.

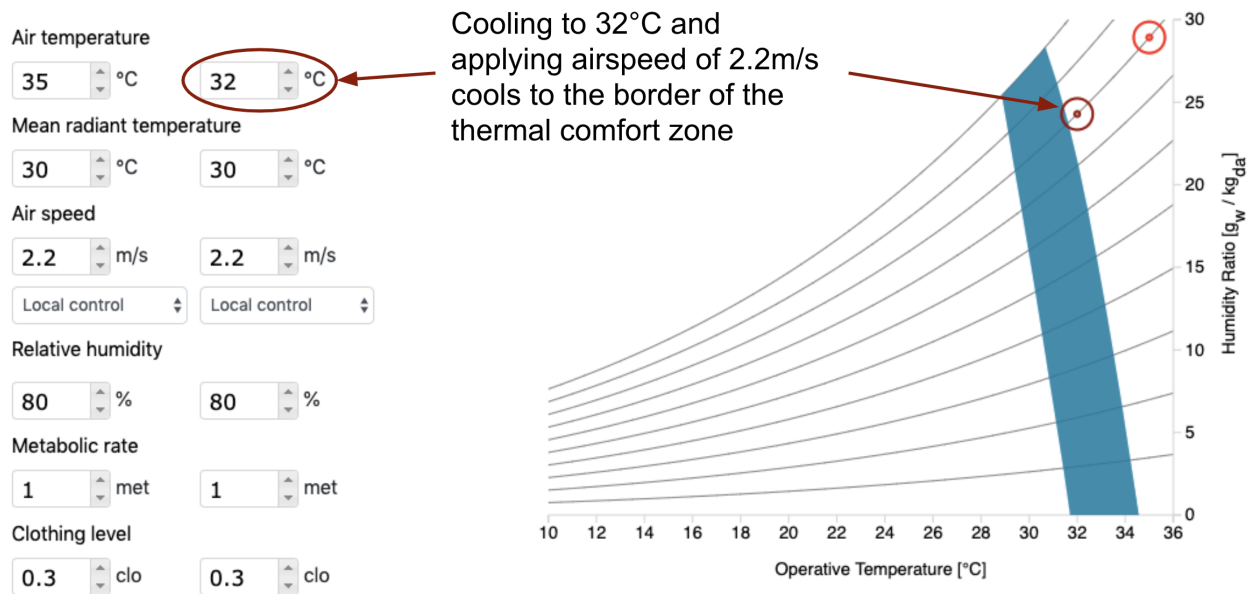


Figure 18: The result generated by the thermal comfort tool shows decreasing air temperature by 3°C at a mean radiant temperature of 30°C, an air speed of 2.2m/s, a relative humidity of 80%, a metabolic rate of 1 met, and a clothing level of 0.3 will cool residents to the edge of the thermal comfort zone.

Thermoelectric Cooling Analysis

Thermoelectric cooling leverages a thermoelectric element or chip that generates a heat flow through p-n semiconductors within the chip when supplied electricity. The heat flow generated by the chip results in a cold side and a hot side. Heat transfer is facilitated by fans which pass air through hot and cold heatsinks. Inlet air either draws heat from the hot side heatsink or loses heat to the cold side heatsink primarily via convection. Hot air is exhausted outside the system and cold air is blown out at a decreased temperature from the ambient air. Figure 19 illustrates how the device leverages the thermoelectric elements to transfer heat between airstreams.

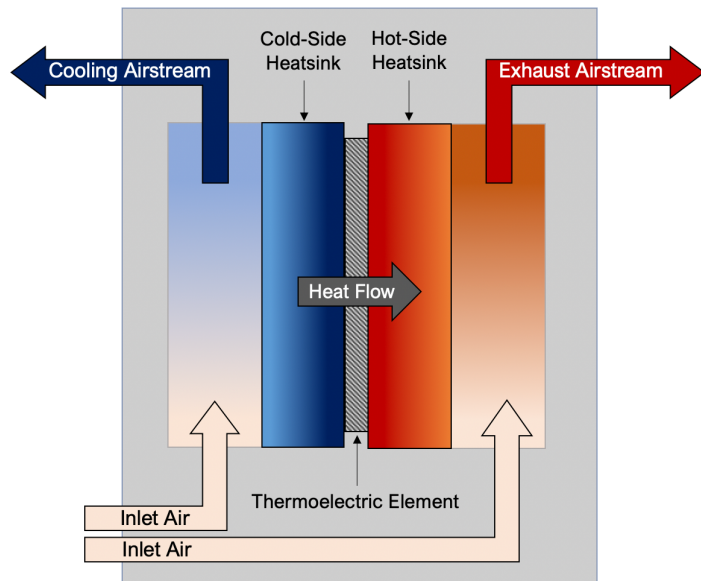


Figure 19: A diagram illustrating the air and heat flows inside the thermoelectric cooling system. When electricity is supplied to the thermoelectric element, it creates a heat flow. The heatsinks improve the heat transfer from the cooling airstream to the exhaust airstream.

An example of a thermoelectric cooling system is shown in Figure 20 below. In this figure, the hot side heatsink is pointing upwards, while the cold side heatsink is pointing downwards. In this configuration the cooling airstream is horizontal, while the exhaust airstream is vertical.



Figure 20: A simple thermoelectric cooling system with cold air output to the left.

A Matlab model was developed to estimate the performance of a thermoelectric cooling system using the system's governing equations. Thermoelectric cooling principles and governing equations are explained in greater detail in the Engineering Analysis of Final Design section of the report (pg.22). From the Matlab model, key parameters such as cooling power, temperature drop of air stream, power input, and coefficient of performance were determined for a given input configuration.

The model was used to estimate the cooling power of a simple thermoelectric cooling prototype. A graph of cooling power, power consumption, and outlet temperature against input current was created for this configuration. This graph is shown in Figure A.1 in Appendix A. The results obtained for this configuration, given an input current of 4.8A through the thermoelectric chip and an air speed of 2.2 m/s, were a cooling power of 46.1 W, a temperature drop of 5.1°C, and a coefficient of performance of about 120%. These results are summarized in Table A.1 found in Appendix A.

Pugh Chart

From the morphological chart, it was evident that the final solution to improving the thermal comfort of residents would be a combination of multiple concepts. Concepts that aim to reduce temperature, reduce humidity, and increase air speed were combined into several possible concept combinations. The combinations were narrowed down to combinations that had the greatest probability of meeting the defined user requirements and engineering specifications. These combinations were placed in the first column of the Pugh Chart shown in Table 6 (pg. 17). The Pugh Chart systematically rates how well each concept meets the user requirements relative to a selected baseline solution. Each user requirement is weighed according to its importance. The Pugh Chart's selected baseline concept combination was a VCRC with an additional fan. This made scoring other concept combinations less challenging as the VCRC is a well-documented cooling solution.

Table 6: A Pugh Chart comparing several possible concept combinations. A larger version of this Pugh Chart is reproduced in Table B.1 in Appendix B to improve visibility.

| | | | Requirement | Safe | Affordable | Adequate Cooling Ability | Compatibility with House Types | Easily Operated | Easily Installed | Durable | Reliable | Easily Repaired or Replaced | Score | Score |
|--|----------------------------|--------------------------|---------------|-------------|------------|--------------------------|--------------------------------|-----------------|------------------|---------|----------|-----------------------------|-------|-------|
| Plausible Concept Combinations | | | WEIGHT (1-10) | 10 | 10 | 10 | 7 | 7 | 7 | 7 | 8 | 6 | 4 | |
| | Temperature | Humidity | Air Speed | TOTAL SCORE | Score | Score | Score | Score | Score | Score | Score | Score | Score | |
| Vapor Compression Refrigeration Cycle | - | Fan | | 0 | 0 | 0 | 0 | 0 | 0 | 0 | 0 | 0 | 0 | |
| Absorption Refrigeration Cycle | - | Fan | | -30 | 0 | -1 | -1 | 0 | 0 | -1 | -1 | 0 | 3 | |
| Direct Evaporative Cooling | Desiccant Dehumidification | Fan | | 25 | -2 | 1 | -1 | 1 | -2 | 2 | 2 | 2 | -1 | |
| Direct Evaporative Cooling | Desiccant Dehumidification | Ceiling Fan Modification | | -5 | -2 | 2 | -2 | 2 | -2 | -2 | 1 | 2 | 0 | |
| Direct Evaporative Cooling | - | Fan | | 66 | 0 | 3 | -1 | 0 | -2 | 2 | 2 | 2 | 1 | |
| Indirect Evaporative Cooling | - | Fan | | 53 | 1 | 0 | -1 | 0 | -1 | 2 | 2 | 2 | 1 | |
| Indirect Evaporative Cooling | - | Ceiling Fan Modification | | 10 | -1 | 1 | -2 | 2 | -1 | -2 | 1 | 2 | 1 | |
| Thermoelectric Cooling | - | Fan | | 84 | 1 | 1 | -1 | 2 | 1 | 1 | 2 | 2 | 1 | |
| Thermal Chimney | - | Fan | | 20 | 1 | 2 | -1 | -2 | 1 | -2 | 1 | 1 | 0 | |
| - | - | Portable Handheld Fan | | 58 | 0 | 3 | -3 | 3 | 2 | 3 | 0 | 0 | -1 | |
| High Reflectivity, Low Absorptivity Tarp | - | - | | 52 | 3 | 0 | -2 | -1 | 3 | -2 | 0 | 3 | 0 | |
| - | - | Thermal Chimney | | 38 | 1 | 2 | -2 | -2 | 3 | -2 | 1 | 2 | 0 | |
| - | Indoor Plants | - | | -39 | 3 | 3 | -3 | 0 | -2 | -1 | -2 | -3 | 2 | |

The concepts above the solid black bar are active, as they require a power source, and the concepts below the bar are passive. The highest scoring active solution combination was a thermoelectric cooling system paired with a fan. The highest scoring passive solution was the high reflectivity, low absorptivity tarp. Upon further consideration of the feasibility of each of these solutions, the thermoelectric cooling system supplemented with fan ventilation was chosen as the final design solution. The high reflectivity, low

absorptivity tarp was found to be too expensive relative to the cooling it provided.

Note: Due to COVID-19 empirical testing, prototyping, and physical validation was cancelled after Week 10 of this 15-week project. The sections beyond this point reflect the work completed given these circumstances.

Final Design Solution

A final design solution was developed to address the need for a low-cost residential climate control system for Bangladeshi slums. The system uses multiple thermoelectric elements to cool an airstream that is directed to the core of users' bodies. Another airstream rejects heat from the unit and delivers it outside the house. A schematic of the cooling process is shown in Figure 21 below.

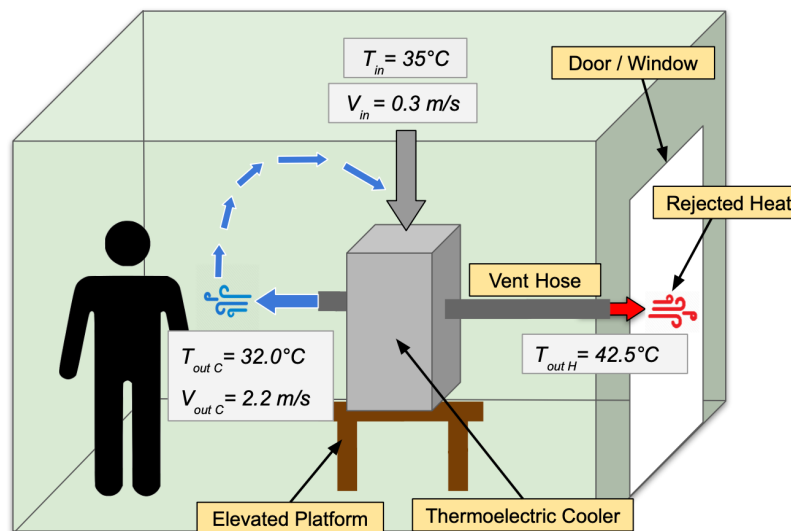


Figure 21: A cooling schematic of the final design showing airstreams and relevant properties.

The final design has four thermoelectric elements that are mounted between two heatsinks: a cold side heatsink, and a hot side heatsink. Air is forced through the heatsinks by two large fans in order to increase cooling power. This system reduces air temperature without increasing relative humidity. Also, the cooling effect of the reduced air temperature is complemented by the cooling effect of the airstream's velocity.

Since prototyping and testing was not possible, a Matlab model of the system was developed to predict its performance. The model was also used to determine the combination of components and system parameters that would yield the best performance. More detail about the Matlab model and the analysis of the thermoelectric cooling system is provided in the Engineering Analysis of Final Design section of the report (pg. 22). A CAD model of the cooling system was created using the components that yielded the best performance. The CAD of the final cooling system is shown in Figures 22 and 23 (pg.21).

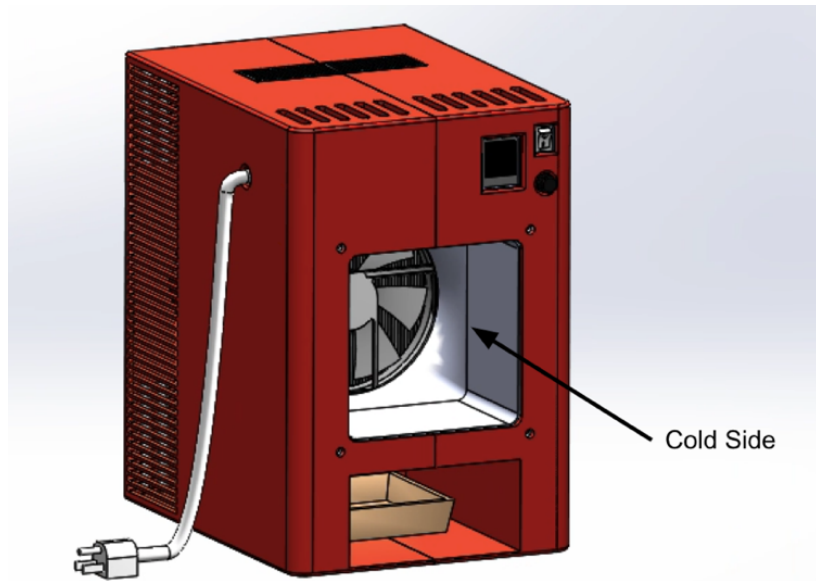


Figure 22: A CAD rendering of the final design solution: a compact thermoelectric cooling system.

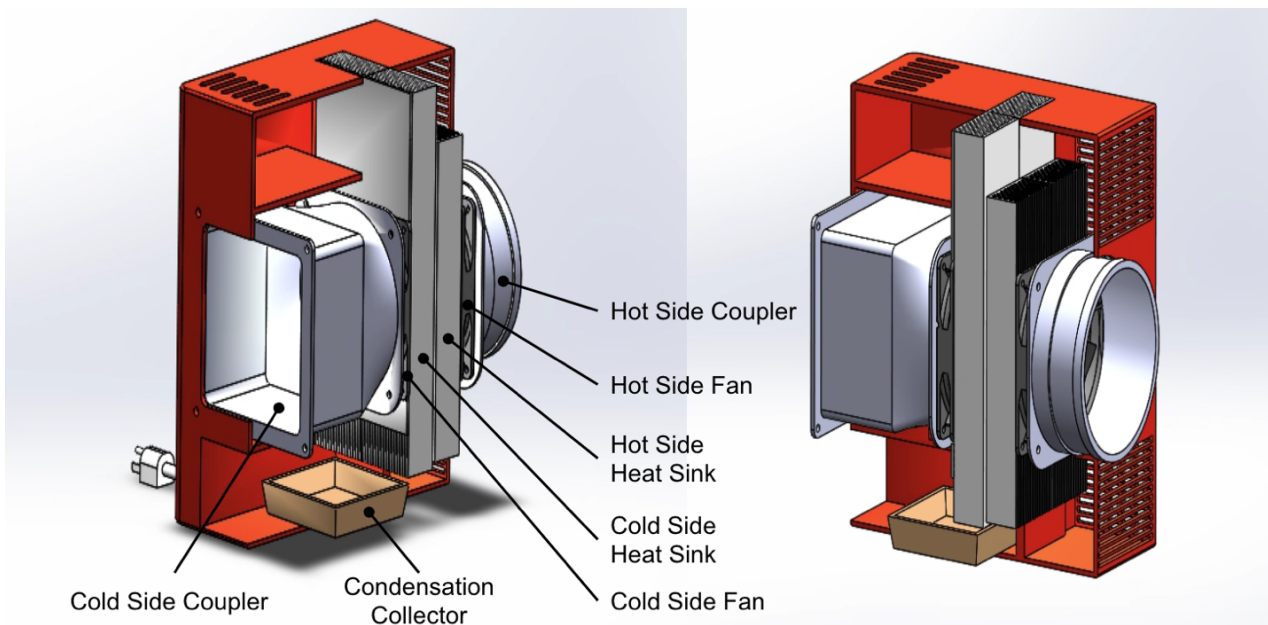


Figure 23: Isometric views of the final design (left and right) showing a detailed breakdown of components and their locations.

The final design has two 14 cm x 14 cm fans, a 300 cm long cold side heatsink, and a 250 cm long hot side heatsink. A condensation collector is placed inside the main housing to collect any water that condenses on the cold side heatsink mounted vertically and drips downward. A large hose or tube can be connected to the hot side coupler to remove the hot exhaust air from the residence. An exploded view of the product can be seen in Figure C.1 in Appendix C.

Engineering Analysis of Final Design

This section of the report provides a complete description of the analysis conducted of the final design solution. The following key elements are discussed:

Thermoelectric Cooling Analysis

- Parameter Identification
- Governing Equations and Calculations
- Convective Resistance – Cold Side Fins
- Convective Resistance – Hot Side Fins
- Fin Efficiency
- Fin Dimension Analysis
- Cooling Performance Analysis
- Correlation with Computational Fluid Dynamics (CFD) Simulation

Cost Analysis and Estimation

- Device Cost Analysis
- Operating Cost Analysis

Thermoelectric Cooling Analysis

This section of the report details the governing equations, calculations, and simulation used to analyze the performance of the final design solution.

Parameter Identification: Thermoelectric cooling leverages a thermoelectric element or chip that generates a heat flow when supplied electricity. This heat flow is related to the cooling power and cooling ability of the system. Mathematical models of the thermoelectric chip can compute cooling and heating power using the primary variables shown in Table 7 below.

Table 7: Key variables used to model the performance of the thermoelectric chip.

| Variables | Definition |
|-------------|--|
| α_s | Seebeck Coefficient (Positive or Negative) |
| ρ_e | Density of p-n junction material |
| K | Thermal Conductivity of p-n junctions |
| N_{TE} | Number of p-n junction pairs within chip |
| L | Height of p-n junctions |
| A_k | Cross section area of p-n junctions |
| J_e | Operating current of thermoelectric chip |
| $R_{k,H-c}$ | Thermal resistivity of thermoelectric chip |
| $R_{e,H-c}$ | Electrical resistivity of thermoelectric chip |
| T_H | Hot side surface temperature of thermoelectric chip |
| T_C | Cold side surface temperature of thermoelectric chip |
| Q_H | Heating power released from thermoelectric chip |
| Q_C | Cooling Power drawn from thermoelectric chip |

A thermoelectric chip contains pairs of positive-negative semiconductor junctions, also known as p-n junctions, that provide cooling and heating on opposite ends when current flows through. This is illustrated in Figure 24 below.

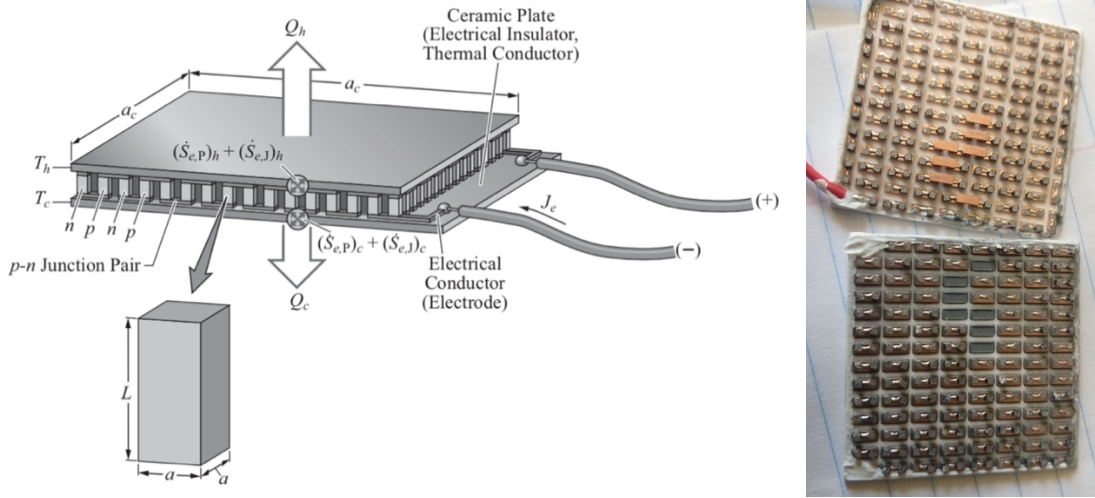


Figure 24: Illustration of a thermoelectric element with pairs of p-n junctions [36] (left) and an image of a TEC1-12706 thermoelectric chip that is broken apart [41] (right).

The physical parameters of the thermoelectric chip can be calculated using Equations 10, 11, and 12 below.

$$\alpha_s = \alpha_{s,p} - \alpha_{s,n} \quad (10) [36]$$

$$R_{e,H-C} = \left(\frac{\rho_e L}{A_k} \right)_p + \left(\frac{\rho_e L}{A_k} \right)_n \quad (11) [36]$$

$$R_{k,H-C} = \left(\frac{A_k K}{L} \right)_p + \left(\frac{A_k K}{L} \right)_n \quad (12) [36]$$

Physical measurements were taken by breaking apart multiple thermoelectric chips, namely TEC1-12706 and TEC1-12710. Other constants were determined from sources [36] characterizing Bismuth-Telluride, which is the material of the p-n junction in this case. These key parameters for TEC1-12706 and TEC1-12710 is shown in Table A.2 found in Appendix A.

Governing Equations and Calculations: The governing energy balance equations of a thermoelectric chip are described by Equations 13 and 14 below. The main components of the energy balance equation are conductive heat transfer between the hot and cold side, Seebeck cooling or heating due to thermoelectric effects [36], and electrical resistance resulting in Joule heating. These components are the first, second, and third terms shown in the equations below.

$$Q_H = - \left(\frac{T_H - T_C}{R_{k,H-C}} \right) + N_{TE} \alpha_s J_e T_H + \frac{1}{2} N_{TE} R_{e,H-C} J_e^2 \quad (13) [36]$$

$$Q_C = \left(\frac{T_H - T_C}{R_{k,H-C}} \right) - N_{TE} \alpha_s J_e T_H + \frac{1}{2} N_{TE} R_{e,H-C} J_e^2 \quad (14) [36]$$

Heat transfer is facilitated by fans which pass air through hot and cold heatsinks. The thermal circuit shown in Figure 25 below illustrates how the device leverages the thermoelectric elements to transfer heat via heatsinks. The terminology used in the figure is listed Table 8 below.

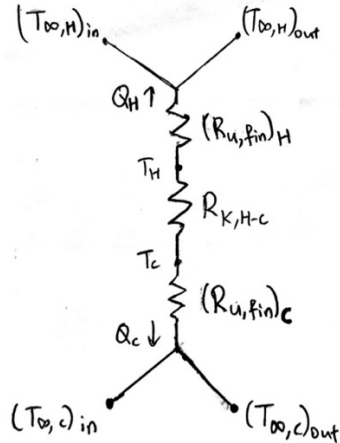


Figure 25: Thermal circuit of heat transfer between the hot and cold chamber of final design

Table 8: Definition of terminology used to model the performance of the thermoelectric chip.

| Variables | Definition |
|------------------------|---|
| $(T_{\infty,H})_{in}$ | Inlet air temperature on hot side |
| $(T_{\infty,H})_{out}$ | Outlet air temperature on hot side |
| $(T_{\infty,c})_{in}$ | Inlet air temperature on cold side |
| $(T_{\infty,c})_{out}$ | Outlet air temperature on cold side |
| $(R_{u,fin})_H$ | Thermal resistivity of hot side heatsink |
| $(R_{u,fin})_c$ | Thermal resistivity of cold side heatsink |

An example of a physical prototype that was acquired prior to the COVID-19 announcement to stop prototyping efforts is shown in Figure 26 below. In the figure, the cold side of the thermoelectric element is facing the small heatsink that points upwards, while the hot side of the thermoelectric element is facing the larger heatsink that points downwards.

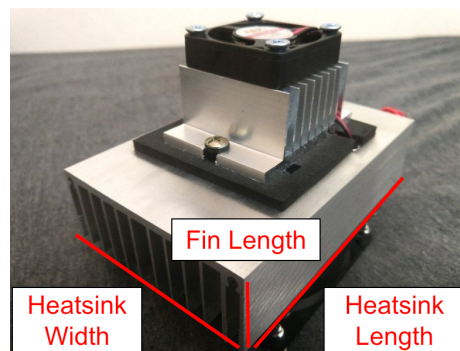


Figure 26: Thermoelectric cooling unit with the heatsink width, heatsink length, and fin length labeled.

Convective Resistance – Cold Side Fins: The cold side of the thermoelectric system was modeled as internal flow where air is forced through openings of the fins that are capped with a layer of insulation. The purpose of such an arrangement is to allow for maximum heat to be transferred from the airstream to the fins when air is flowing through these openings. An example of this is illustrated in Figure 27 below.



Figure 27: Convective heat transfer of air stream on cold side modelled as internal flow.

Firstly, the hydraulic diameter of each opening, D_h , was computed using the cross-section area, A_u , and perimeter, P_{ku} , for each opening shown in Equation 15 below.

$$D_h = \frac{4A_u}{P_{ku}} \quad (15) [36]$$

Reynolds number, $Re_{D,h}$, was then calculated using parameters such as air speed through the cold side fins, $(U_\infty)_C$, kinematic viscosity of air, $\nu = 1.57e-5 \text{ m}^2/\text{s}$ [36], and the abovementioned hydraulic diameter, D_h . This is shown by Equation 16 below.

$$Re_{D,h} = \frac{U_\infty D_h}{\nu} \quad (16) [36]$$

An approximation for the Nusselt's number was made using the formula for air flowing through a rectangular channel using $Re_{D,h}$ and Prandlt Number, $Pr = 0.69$ [36], as shown in Equation 17 below.

$$Nu_{D,h} = 0.023 Re_{D,h}^{4/5} Pr^{0.3} \quad (17) [36]$$

The local convective resistance was then calculated using Equation 18 below, where thermal conductivity is $k_f = 0.0267 \text{ W/mK}$.

$$R_{ku} = \frac{D_h}{A_u Nu_{D,h} k_f} \quad (18) [36]$$

Since the temperature of air is continuously decreasingly as it flows through the rectangular heatsink channel, there was a need to find the average convective resistance of the heatsink, R_u , using the Number of Transfer Units (NTU) analysis. First, NTU was calculated using Equation 20 below, where $c_p = 1005 \text{ J/KgK}$ refers to the specific heat capacity of air. The mass flow rate of air, \dot{m} , was calculated using Equation 19 below.

$$\dot{m} = A_u U_\infty \quad (19) [36]$$

$$NTU = \frac{A_u Nu_{D,h} k_f}{D_h \dot{m} c_p} \quad (20) [36]$$

Next, the heat exchange effectiveness, ϵ_{he} , was then calculated using Equation 21 below.

$$\epsilon_{he} = 1 - e^{NTU} \quad (21) [36]$$

Finally, the average convective resistance, R_u , was computed using Equation 22 below.

$$R_u = \frac{1}{\dot{m}c_p\epsilon_{he}} \quad (22) [36]$$

Convective Resistance – Hot Side Fins: The hot side of the thermoelectric system was modeled as semi-bounded flow where air flows through openings of the fins that are not covered. The purpose of such an arrangement is to allow for maximum heat to be dissipated from the heatsink such that cooling power on the cold side can be maximized, as seen from the governing energy balance Equations 13 and 14 (pg.23) [36].

The local convective resistance, R_{ku} , was calculated using the abovementioned Equations 15 to 17. However, unlike the analysis for the cold side, Equation 17 was altered to the more appropriate approximation for Nusselt's number for semi-bounded convection. This is shown by Equation 23 below.

$$Nu_{D,h} = 0.664 Re_{D,h}^{1/2} Pr^{1/3} \quad (23) [36]$$

Another distinction from the cold side convective resistance analysis is that there is no need to compute the average convective resistance. This is because the temperature of air through the fins is assumed to be constant. Therefore, it is sufficient to compute the local convective heat resistance, R_{ku} (Equation 18).

Fin Efficiency: The temperature distribution through the fins is not uniform due to conductive resistance. The fin efficiency, η_{fin} for both fin arrays is described by Equations 24-26 below, where L_{fin} , t_{fin} , L_c , m refers to the length, thickness, corrected length of square fins. m is a measure of extinction of fin temperature.

$$L_c = L_{fin} + \frac{t_{fin}}{2} \quad (24) [7]$$

$$m = \frac{1}{L_c} \left(\frac{R_{k,s}}{R_{ku}} \right) \sqrt{\frac{2Nu_{D,h}k_f}{D_h k_s t_{fin}}} \quad (25) [7]$$

$$\eta_{fin} = \frac{\tanh(mL_c)}{mL_c} \quad (26) [7]$$

The overall fin efficiency, η_o , was then described by Equation 27 below, where N refers to the number of fins in the fin array. A_{fin} refers to the total area of fins alone while A_t refers to the total exposed surface area including fin and base.

$$\eta_o = 1 - \frac{NA_{fin}}{A_t} (1 - \eta_{fin}) \quad (27) [7]$$

Consequently, two additional heat transfer equations were formulated to relate thermoelectric element surface temperature with inlet air temperature through the fins, as shown in Equations 28 and 29 (pg.27). It is important to note that Equation 28 uses local convective resistance R_{ku} for the semi-bounded flow while Equation 29 uses average convective resistance R_u for the internal flow.

$$Q_H = \eta_{fin,H} * \frac{T_H - (T_{\infty,H})_{in}}{(R_{ku})_H} \quad (28) [7]$$

$$Q_C = \eta_{fin,C} * \frac{T_C - (T_{\infty,C})_{in}}{(R_u)_C} \quad (29) [7]$$

Combining these equations with Equations 18, 22, and 26 above, yields the 4 equations that were used to determine the unknowns T_H , T_C , Q_H , Q_C .

After calculating Q_C , the outlet air temperature, T_{out} , input power, P_{input} , and Coefficient of Performance, COP , were calculated using Equations 30-32 below.

$$(T_{\infty,C})_{out} = (T_{\infty,C})_{in} + \frac{\dot{Q}}{\dot{m}C_p} \quad (30) [7]$$

$$P_{input} = N_{TE} R_{e,H-C} J_e^2 + N_{TE} \alpha_s J_e (T_H - T_c) \quad (31) [7]$$

$$COP = \frac{P_{input}}{P_{output}} \quad (32) [7]$$

Fin Dimension Analysis: From the abovementioned equations, a Matlab model was developed to analyze the entire thermoelectric system. It was first used to analyze how heatsink length, heatsink width, and fin length impact cooling power and outlet temperature for a fixed mass flow rate. These heatsink and fin terminologies are described in Figure 26 (pg.24).

From Figures 28 and 29 below, it is apparent that cooling power increases, but with diminishing increase, with increasing heatsink length or heatsink width. When these parameters are increased, is an increase in contact surface area between the airstream and the fin array, leading to lower convective resistance (Equation 20-22) and hence greater cooling power (Equation 29). However, the increase in these parameters leads to an increase in channel cross-section area which leads to a decrease in air velocity for the same mass flow rate coming from the fan (Equation 19). As a result, Reynold's number (Equation 16) and consequently Nusselt's number decrease (Equation 23), leading to a higher convective resistance and hence lower cooling power (Equation 29). This accounts for the diminishing increase in cooling power as observed.

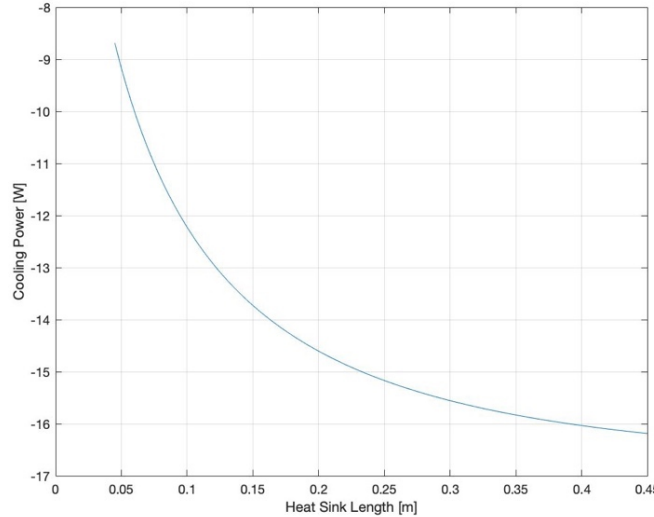


Figure 28: A plot showing the relationship between cooling power and heatsink length.

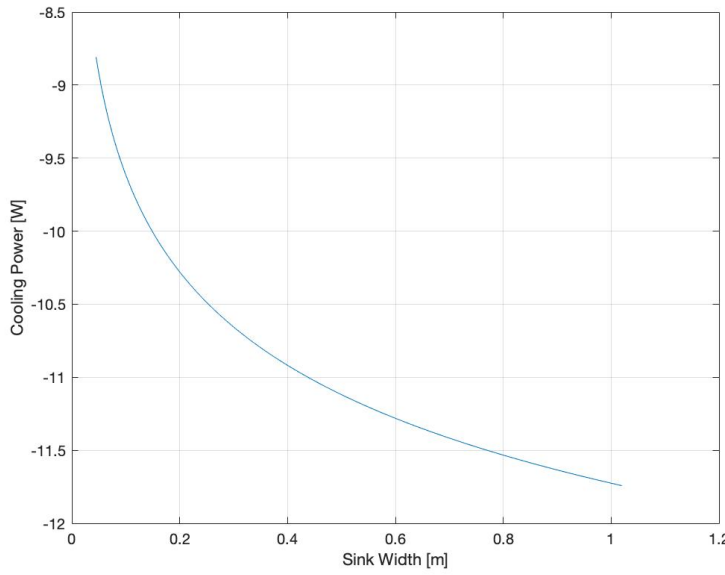


Figure 29: A plot showing the relationship between cooling power and heatsink width.

However, a bell-curve shaped trend is observed instead for the relationship between cooling power and fin length. While similar abovementioned principles apply, an increasing fin length leads to decreasing fin efficiency (Equation 26), leading to a decrease in cooling power (Equation 29). From Figure 30 below, this increasing cooling power trend is reversed at a length of 0.09m.

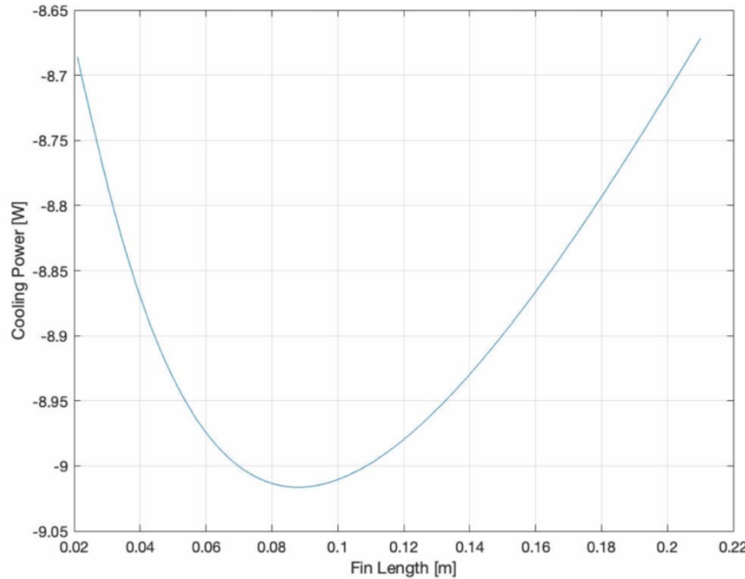


Figure 30: A plot showing the relationship between cooling power and fin length.

These plots reveal that increasing the heatsink length will lead to greater cooling power. Table 9 (pg.29) shows various combinations of fin and fan configurations for both the cold and hot sides of the unit, as well as different thermoelectric elements. Parameters were approximated from descriptions of real-world products sold on Amazon. Changes in configuration are highlighted in green.

Table 9: Summary of the different thermoelectric system configurations explored.

| Config | Cold Side | | Hot Side | | Middle |
|--------|-----------------|---------------------|-----------------|---------------------|-----------------------|
| | Heatsink Length | Fan | Heatsink Length | Fan | Thermoelectric Module |
| 1 | 100mm [42] | 4x4cm – 5 CFM [44] | 100mm [42] | 8x8cm – 45 CFM [46] | TEC1-12706 [48] |
| 2 | 150mm [43] | 8x8cm – 17 CFM [45] | 100mm [42] | 8x8cm – 59 CFM [47] | TEC1-12706 [48] |
| 3 | 150mm [43] | 8x8cm – 17 CFM [45] | 150mm [43] | 8x8cm – 59 CFM [47] | TEC1-12706 [48] |
| 4 | 150mm [43] | 8x8cm – 17 CFM [45] | 150mm [43] | 8x8cm – 59 CFM [47] | TEC1-12710 [41] |

Of the four configurations, Configuration 4 produced the best cooling ability. It is important to note that operating the thermoelectric chip at optimal current of 8.9A yields a temperature drop of 6.4 K but at a poor COP of 43.1%. However, operating at lower current of 4.8A yields a temperature drop of 5.1 K, which still meets our thermal comfort requirement (Table 3), with a superior COP of 120%. Table A.1 in Appendix A shows a summary of the results obtained for Configuration 4.

Cooling Performance Analysis: The cooling performance of the final solution was derived by inputting key parameters of the final design into the Matlab model. Since the thermal circuit behaves like 4 parallel branches, each with 1 thermoelectric chip, it is expected that the system's input power, cooling power, and heating power are 4 times larger than the model's results if 1 thermoelectric chip was analyzed. A graph of cooling power, power consumption, and outlet temperature against input current was generated for this new configuration. This graph is shown in Figure 31 below. Note that the x-axis refers to the current per parallel branch, not total current.

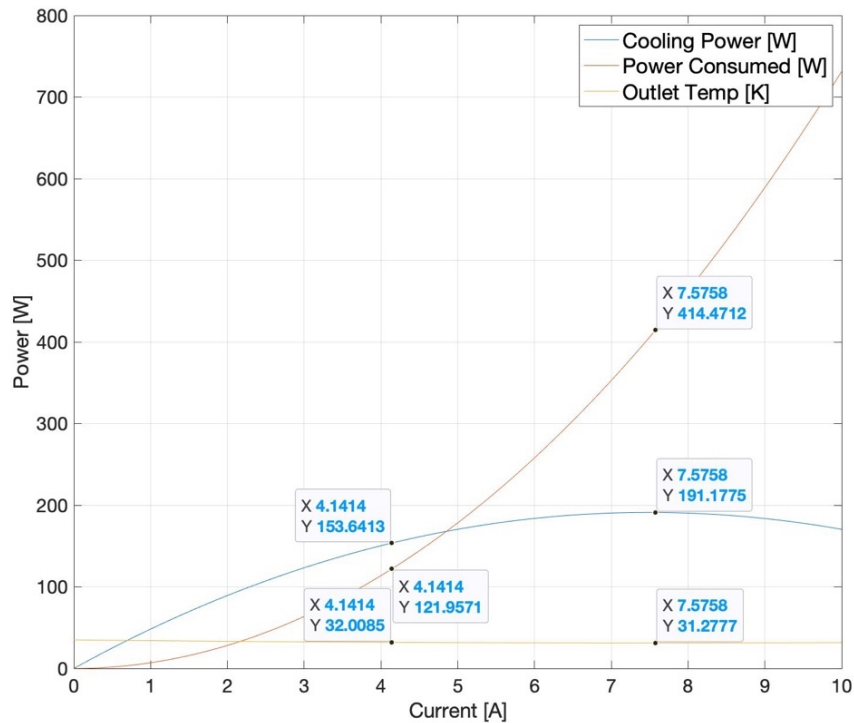


Figure 31: Cooling power, power consumption, and outlet temperature against input current.

From the Matlab model, it was determined that if the final product was operated at ideal COP, it would achieve an air speed of 2.2 m/s through the 14 x14 cm outlet duct, with a temperature drop of 3.0°C. This matches the engineering specifications of 2.2 m/s air speed and 3.0°C of temperature drop shown in Table 3 (pg._). The results are highlighted in Table 10 below.

Table 10: Matlab results of key parameters for final design

| Variables | Symbol | Optimal Current | Higher COP |
|-----------------------------------|--|-----------------|--------------|
| Total Input Current [A] | J_e | 30.6 | 16.6 |
| Power Required [W] | P_{in} | 418.3 | 125.8 |
| Inlet Air Temperature [K] | $(T_{\infty,C})_{in}, (T_{\infty,H})_{in}$ | 308.2 | 308.2 |
| Cold Mass Flow Rate [CFM] | \dot{m}_c | 92.0 | 92.0 |
| Cold Air Speed [m/s] | $(U_{\infty})_c$ | 2.2 | 2.2 |
| Chip Temperature – Cold [K] | T_c | 301.3 | 302.7 |
| Cooling Power [W] | Q_c | 191.2 | 153.6 |
| Outlet Air Temperature - Cold [K] | $(T_{\infty,C})_{out}$ | 304.4 | 305.2 |
| Temperature Drop – Cold [K] | $(\Delta T)_c$ | 3.8 | 3.0 |
| Hot Mass Flow Rate [CFM] | \dot{m}_H | 92.0 | 92.0 |
| Hot Air Speed [m/s] | $(U_{\infty})_H$ | 2.8 | 2.8 |
| Chip Temperature – Hot [K] | T_H | 349.5 | 327.0 |
| Heating Power [W] | Q_H | 605.6 | 275.6 |
| Outlet Air Temperature - Hot [K] | $(T_{\infty,H})_{out}$ | 324.5 | 315.6 |
| Coefficient of Performance [%] | COP | 45.7 | 122.1 |

While the results of the final design look promising, there are a few key assumptions made in the model that might lead to an overestimation of the cooling ability of the product.

Firstly, the model did not consider the pressure drop that would occur when air is drawn and forced through the small openings between the fins. This will result in a decrease in mass flow rate from the fan's nominal mass flow rate, resulting in a lower air velocity than expected. A possible solution to remedy this is the usage of an extra 14x14cm fan stacked atop the existing fan to increase static pressure and hence regain any loss in mass flow rate. Note that mass flow rate will not increase beyond the fan's nominal value of 92 CFM if this method were to be adopted.

Secondly, the Matlab model assumes constant heatsink base temperature, when in reality the 4x4cm thermoelectric chip would only cover a small portion of the heatsink. This would lead to an overestimation of cooling power. A method to remedy this would be to consider using 6 or 8 thermoelectric chips spread out across the base of the heatsink operated at lower current. Even with the same cooling power, this method would result in a higher COP, which is desirable.

Correlation with Computational Fluid Dynamics (CFD) Simulation: The Matlab model was used to estimate the cooling ability of the system and optimize components for the best system performance. However, due to COVID-19 empirical testing could not be conducted to validate this model and corroborate its results. Instead, CFD simulations were developed using ANSYS Fluent to validate the Matlab model. The portion of the Matlab model that the CFD was used to validate was the heat transfer occurring between the cold side heatsink and the air flowing through it.

The hypothesis tested was as follows: given the same heatsink base temperature, airstream velocity, and airstream outlet temperature, the Matlab model and the CFD simulation should compute similar values for the heat flowing through the heatsink's base. Both the Matlab model and the CFD simulation assume that the heatsink base temperature is uniform. To improve the resolution of the CFD simulation, a section of the heatsink was analyzed. The results were scaled to evaluate the entire heatsink.

Through CFD simulation, contour views of a section of the heatsink and airstream were generated. The contour views illustrate the temperature variation in each body and are shown in Figure 32.

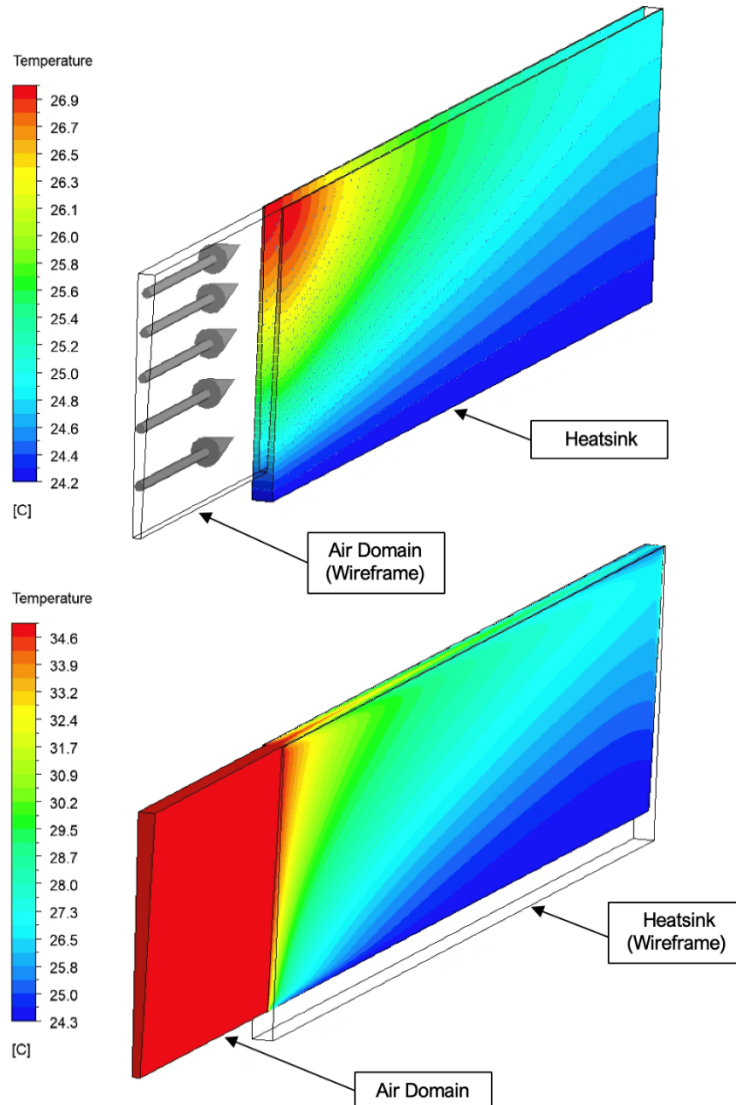


Figure 32: Two contour views illustrating the temperatures of the heatsink (top) and the airstream (bottom). The airstream's contour view shows the gradual formation of a thermal boundary layer.

Using the CFD simulation, the rate of heat transfer through the heatsink's base was determined. A calculation with equivalent input parameters was conducted using the Matlab model. The results of both calculations as well as their input parameters are summarized in Table 11 below.

Table 11: A summary of the results obtained during validation of the Matlab model using a CFD simulation.

| Parameter | Input | Matlab Output | CFD Output |
|--|----------|---------------|-------------|
| Inlet Velocity (m/s) | 4.9 | - | - |
| Inlet Temperature [°C] | 35.0 | - | - |
| Outlet Temperature [°C] | 28.8 | - | - |
| Heatsink Base Temperature [°C] | 24.3 | - | - |
| Heat Flow Through Heatsink Base [W] | - | 58.0 | 62.5 |

The Matlab model and CFD simulation computed a heat flow of 58.0 W and 62.5 W through the heatsink base, respectively. The difference between the two results is 7.7% and may be explained a key difference between the Matlab model and the CFD simulation. The CFD simulation takes entrance region effects into account, while the Matlab model assumes fully-developed flow. The Nusselt number and average convection coefficient are lower for fully-developed flow than for flow through the entrance region. Thus, the CFD simulation may calculate a slightly higher heat flow through the heatsink base than the Matlab model. Despite the slight difference in the results obtained from the two methods, the CFD simulation corroborates the Matlab model's heat transfer calculations for the cold side heatsink.

Cost Estimation and Analysis

It is important that the climate control system is accessible to as many urban slum residents as possible, so the system's cost must be affordable. The cost of the system has two components, the initial device cost and the recurring operating cost. Both of these costs were estimated for the final design solution.

Device Cost Analysis: The bill of materials (BOM) of the final design can be found in Table D.1 in Appendix D. From this BOM the unit cost of the design was estimated assuming a production volume of 10,000 units. The final cost of the unit was estimated to be \$43.34 or 3682 Tk. Although this estimated cost is greater than the target cost of \$25-50 or 2124 - 4248 Tk (Table 3), with further analysis and prototyping the cost can be reduced. Much of the cost of the device is attributed to the plastic casings, which will be manufactured through injection molding. The design of these casings can be optimized for injection molding to reduce cost.

Operating Cost Estimation: The solution is expected to be used 12 hours per day and have the highest demand for the warmest eight months of the year. The final design has an operating power of 126W, and the local electrical rate is 5.33 Tk/kWh. Combining these parameters, the monthly operating cost of the final solution is expected to be 244 Tk/mo. (~1955 Tk/yr.). This operating cost is approximately 65% of the operating cost of a standard refrigerator. The operating cost of the unit may be justifiable if it can effectively cool residents. However, for later design iterations this cost can be reduced by increasing the COP of the system. One method of increasing the COP is to increase the number of thermoelectric elements, while decreasing the current supplied to the elements.

Risk Assessment

Since empirical testing could not be completed for this project, the risk assessment conducted was based upon computational results. The thermoelectric cooling device contains both heating and electrical components, which must be considered not only for analyzing cooling effectiveness, but also for safety. In terms of safety, the hot side heatsink provides concern for burning, because the heatsink is estimated to get up to 65°C. Furthermore, the wires connecting the fans and chip to the power source must be properly insulated so that they do not pose a hazard to users, especially children. Additionally, the insulation must prevent contact with water. These risks can be mitigated by packaging the device appropriately. To meet the engineering specifications, the device must be easily repaired or replaced, while also preventing penetration from water or dust. Therefore, the packaging must conceal the electrical components, but still be modular so that it can be taken apart for maintenance or repair. The packaging design, which serves to optimize performance while mitigating safety risks, is shown in Figures 22 and 23 (pg.21).

In addition to safety risks, there are performance-based risks involving the efficiency of the cooling system. There is a concern regarding properly exhausting the hot air outside the residence to prevent the hot air from mixing with the ambient air. This would result in decreased performance because it would raise the temperature of the air input into the device, resulting in less cooling and wasted energy. Therefore, it is crucial that this design uses insulated tubing to direct the exhaust heat outside. This tubing must be long enough to reach outside a door or window while still allowing the device to be located at a desirable location within the residence to maximize cooling throughout the room.

Finally, there is an additional risk for condensation building on the cold side heatsink from the water vapor in the air. Though freezing is not a concern due to the temperature of the heatsink, the buildup of liquid on the fins could decrease performance by disrupting airflow, causing rust to form, and creating pools of water. To mitigate this concern, the fin orientation of the cold heatsink was rotated 90° so that the fins are perpendicular to the ground, allowing condensed water droplets to flow down into a collecting plate. This design change is reflected in the CAD model shown in Figure 23 (pg. 21).

With these changes, the highlighted risks and safety concerns - decreased efficiency due to hot air recirculating and condensation buildup - will be mitigated to an acceptable level. Additional testing in the future using DMFEA analysis and user testing will further ensure these risks are avoided.

Validation

Validation and verification are essential parts of the design process. Since the development of the cooling solution took place very far from the end users in Rayer Bazar, only verification of the solution has been accomplished to date. However, it is paramount to the success of this project that the solution be both verified and validated, so a plan has been constructed detailing how to do so in the future. This plan can be seen via the flowchart in Figure 33 (pg.35). This flowchart covers both what is planned, as well as what has been completed to date with regards to both the verification and validation of the solution.

Due to the COVID-19 pandemic, all physical prototyping and experimentation had to be replaced with virtual analysis. Matlab, Ansys Fluent, and SolidWorks were leveraged to complete as much verification of the engineering specifications as possible.

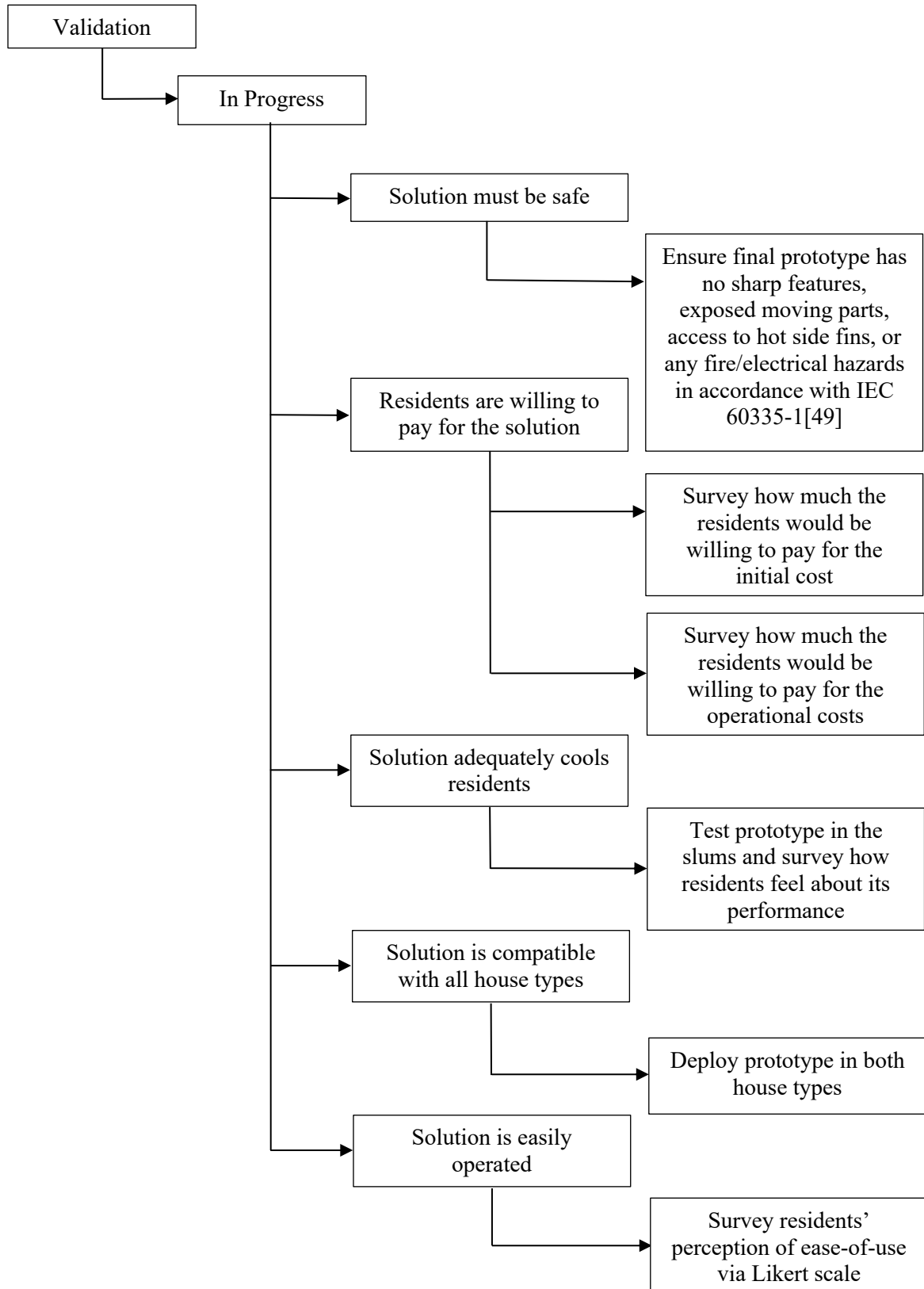
During concept selection, a Matlab model was created to better understand the capabilities of a thermoelectric solution. It was created with the help of Professor Massoud Kaviany's understanding of thermoelectric cooling and governing equations from his heat transfer textbook [36]. From this script, it was determined that a thermoelectric solution could provide adequate cooling of 58.0 W, satisfying the requirement of adequate cooling. During this process, various system parameters were refined to

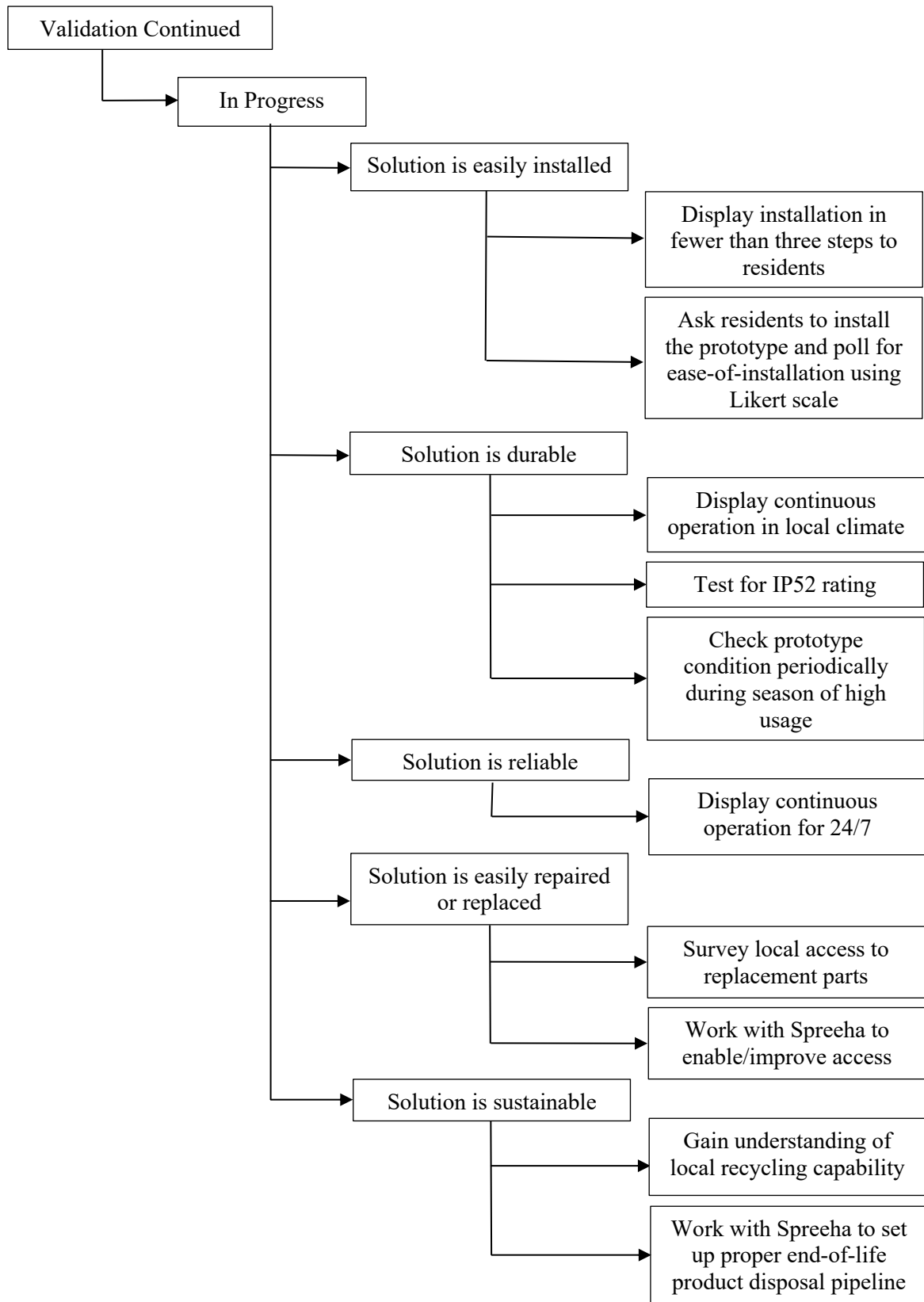
maximize cooling power. Heatsink fin dimensions, voltage applied to the thermoelectric chips, and the flowrate of air through the system were all variables that needed to be optimized to achieve maximum cooling. The Matlab model allowed for virtual analysis of how these variables could affect the cooling power of the system and aided in choosing the final system parameters. The model also allowed the performance of the final design solution to be estimated.

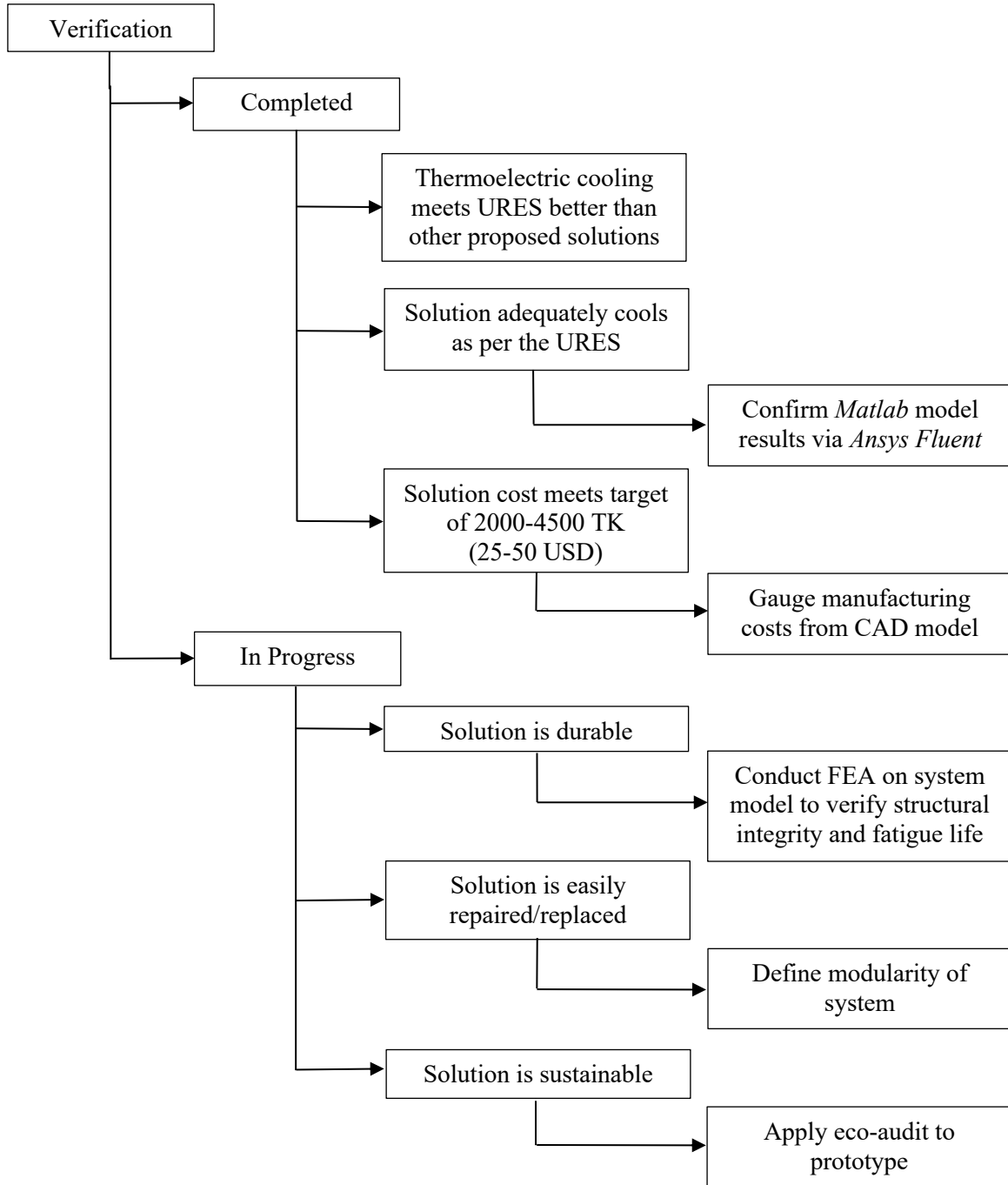
Computational fluid dynamics (CFD) via Ansys Fluent was conducted on the cold side heatsink to corroborate the results obtained from the Matlab model. A contour map of a single fin within the cold side heatsink can be seen in Figure 32 (pg. 31). The results in cooling power between the two models differed by 7.7%, with the CFD model predicting a slightly higher cooling power of 62.5 W. The CFD analysis was conducted with the aid of Julio Ferreira, a graduate student working under Professor Massoud Kaviany. The parity between the Matlab model and CFD model serves as justification that a real-world prototype will provide adequate cooling power as per the user requirements and specifications (URES).

A CAD model of a potential prototype was created using SolidWorks and can be seen in Figure 22 (pg. 21). From this model, a preliminary system cost of \$43.34 was calculated using component costs found from real-world suppliers. This price is within the cost range of \$25-50 and can be further improved upon in the future once a prototype is built. Possibility of subsidization has not been fully considered due to time constraints and the fact that a prototype is not yet built. Therefore, this virtual estimation of the solution's cost acts as the verification of the affordability requirement. Possible funding sources are likely to be explored, and relevant design improvements are likely to be made in the future to further drive down the cost.

Figure 33: Validation and Verification plan for the thermoelectric solution.







To validate the system, a prototype will need to be constructed and tested in Bangladeshi urban slums. As seen in Figure 33 (flowchart), the prototype plays a main role in validating the design. It is paramount that the residents have first-hand experience using the prototype to assess its satisfaction of their needs. An in-depth understanding of their installment, use, and eventual disposal of the solution can only be achieved if the prototype is in their hands. For the surveying mentioned in Figure 33 (flowchart), it is important to poll as many kinds of residents as possible to ensure that they can comfortably use the solution, regardless of their age or physical ability. To standardize the process, polling should be done via a Likert scale. BLUElab Bangladesh will be carrying on this project and has travelled to Rayer Bazar in the past to gather the residents' need statements. Fabricating a prototype and testing it in the field is something that BLUElab has the resources to accomplish and is the best way to validate the design.

Prior to validation, it is key that the prototype be tested via real-life experiments. Before the COVID-19 pandemic, a control volume was designed to test various cooling solutions. It consists of an insulated plastic bin with holes for inlet and outlet air flows as well as thermocouples. A CAD model of this system and test set up can be seen in Figure 34 below. A test procedure was created to accompany the system and can be seen in Table 12 below. The test plan was finalized with the aid of John Laidlaw, an engineering technician in the G.G. Brown Laboratory. Replicating conditions commonly seen in Rayer Bazar within the control volume will add value to the results of prototype testing, as opposed to testing it in the local Michigan climate and extrapolating results. The test plan and the design of the test environment will be passed on to the BLUElab Bangladesh team for further consideration and realization.

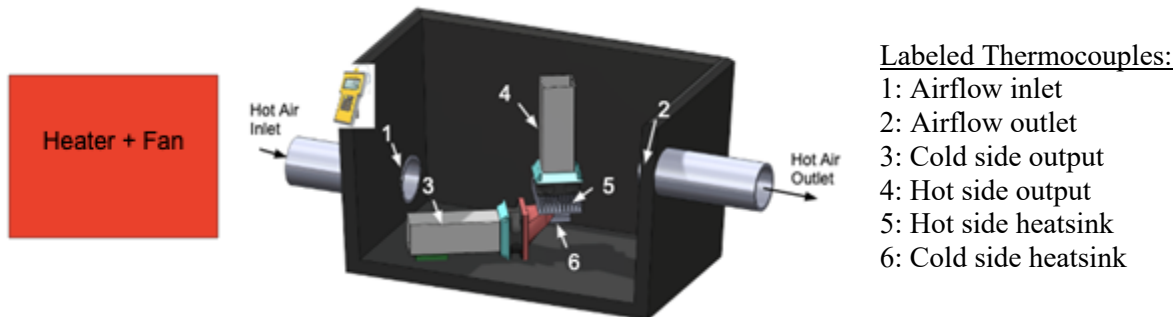


Figure 34: Test setup with labeled thermocouple locations.

Table 12: Preliminary testing procedure of thermoelectric device.

| Step | Procedure |
|------|--|
| 1 | Arrange thermocouples as shown in the test setup figure. |
| 2 | Turn on heater (HIGH setting). Face heater towards the hot end PVC pipe outside the control volume. Start with the heater about 5 inches away from the PVC pipe opening. |
| 3 | Monitor the temperatures of thermocouples 1 and 2. Wait until the thermocouple temperatures at BOTH in the inlet and outlet of the control volume reach 38-40 °C. The distance between the heater and the inlet pipe may need to be adjusted. |
| 4 | Measure the initial temperatures of thermocouples 3, 4, 5, and 6. Record. |
| 5 | Turn on the thermoelectric cooler by supplying 12V to the two fans and the thermoelectric element using an external power supply. |
| 6 | Take measurements of thermocouples 3, 4, 5, and 6 every 30 seconds for the first 5 minutes, and every minute after until the temperatures stabilize for three consecutive readings. These measurements will monitor temperatures of the hot and cold output air flow, as well as the temperatures of the hot and cold heatsinks. |

Discussion and Recommendations

Reflecting back on this design process, one thing we would have done differently is spend less time focused on evaporative cooling as a potential solution. While this concept is affordable, sustainable, and passive, it adds humidity to the system and is less effective in humid climates. Knowing that we were designing for a humid climate, we should have ruled out this solution earlier in the process so we could have had more time to work on our thermoelectric cooling solution.

A strength of our solution is that it is able to decrease air temperature without increasing humidity. This temperature drop was predicted by a Matlab model which was verified by CFD analysis. Additional strengths of our final solution include being compact, easy to transport, and easy to install non-invasively. Furthermore, the thermoelectric cooling unit does not require daily maintenance or extra resources such as water to function. Design weaknesses include requiring power from the grid, which increases cost to the user, and requiring hot air to be expelled through a pipe outside the residence. In addition, due to inability to test for validation, it is unclear whether or not a user will actually be adequately cooled to their comfort level. Finally, the packaging constraints add to the total cost of the product and may reduce efficiency.

One recommendation that could be implemented in a future design iteration is onboard collection and storage of ambient temperature and device usage data. This data could be used to further improve our understanding of the conditions inside residences as well as the extent to which the device is used. Analysis of this data would be useful to verify the user requirements and engineering specifications. Additionally, we recommend that our sponsors (BLUElab members and Spreeha) continue with validation testing in Bangladesh once it is safe to do so. To ensure successful implementation of this solution for years to come, we also advise that they work with local suppliers and workers to increase access to replacement parts. Finally, it is important that there is access to proper recycling of parts where applicable to ensure sustainability for the entire lifetime of the device.

Ethics and Professional Responsibility

As engineers, there is a responsibility to report accurate results, prioritize safety, and conduct proper testing before releasing a product to the market. The Code of Ethics has been closely followed for this project to ensure transparency, accurate analysis and proper verification.

The first ethical consideration for the cooling comfort system is the prioritization of safety. Mitigating risks such as burning, electrical fires, or sharp edges does not directly improve the cost-effectiveness of the design, but it is critical to the success of the design. In addition, during analysis with the Matlab model and CFD simulations, it was important to report accurate results, even if those results fell short of our engineering specifications. For example, evaporative cooling was the leading concept that was further analyzed earlier in the design process. While this solution appeared to provide sufficient cooling based on its ability to decrease temperature, it would also increase humidity. This increased humidity would have decreased cooling comfort in an already humid climate. Humidity is a metric that is less obvious than temperature, but academic literature indicates that it is equally important to consider when analyzing thermal comfort. Therefore, even though it required more work to find and analyze another concept, it was the correct ethical decision to make to ensure the design is not only effective on paper, but in real life.

Engineers have an obligation to provide results and present them in an objective manner. Therefore, it was important to adhere to the engineering requirements and specifications when choosing between multiple concepts, rather than choosing a concept that may have appeared less complicated or seemed subjectively more favorable. Throughout this process this design team was committed to being honest with each other and our advisor, Professor Kaviani, so that decisions could be made ethically and

responsibly. This design project was motivated by our desire to serve the public and improve the quality of life of our end users.

Sustainable Design Assessment

The first consideration when evaluating if a design is sustainable is to determine if it addresses an unmet environmental or social challenge. The thermoelectric cooling system was designed to improve the thermal comfort of residents in an urban slum in Bangladesh. Interviews and preliminary research conducted by BLUElab members have identified thermal comfort as an unmet need in the area. Temperature, humidity, and airflow were identified as the three components that must be considered when assessing thermal comfort. Current solutions involving weak ceiling fans are not sufficient. Through engineering analysis and verification, the thermoelectric cooling solution makes progress towards the unmet need. Based on modeling, the system will decrease the temperature and increase the airflow around residents without increasing humidity.

The second concept of sustainable design is ensuring the design will not lead to undesirable consequences in its lifecycle that outweigh its intended benefits. To address this aspect of sustainability, possible safety hazards were identified so that they could be mitigated. These hazards include burning from the hot side of the thermoelectric unit, electrical complications due to water exposure, unshielded moving parts, and sharp edges. Packaging was designed to protect the users from these potential harms. Furthermore, to reduce harmful effects to the environment, single-use plastics were not selected to be used for any components of this design.

In addition, this design was developed to not only be affordable for the residents of Rayer Bazar, but also to ensure that it will be adopted and self-sustaining in the market. While the low-cost requirement introduced significant design constraints, it is crucial that the cost of the solution be affordable for the residents so that it can continue to be implemented for years to come. The final cost o

f this solution is estimated to be \$43.34 or about 3682 Tk. With the possibility of subsidies and cheaper manufacturing, the goal is to further decrease this cost in the future. Based on the cost benchmarking of existing cooling devices (such as current ceiling fans and refrigerators), we believe our solution can be sustainable in the low-resource market.

The final consideration of sustainable design involves ensuring that planetary or social systems are not worse off economically due to the design. Since the solution is not made for profit and given that there are no competing devices, there is no anticipation that the sales of this solution will have any detrimental effects to the economy or hurt existing businesses. Furthermore, many of the materials chosen for the prototype are recyclable. ABS plastic for the packaging of the thermoelectric system is recyclable, and the heatsinks are made of aluminum, a material that is 100% recyclable. Bangladesh currently has many companies that recycle scrap materials and connecting the Rayer Bazar population with these resources will be important in the future, as seen in the validation plan in Figure 33 (pg. 35-37).

Engineering Standards

Engineering standards are important in ensuring the safety and welfare of users, as well as in providing engineers with proven guidelines and test plans. Engineering standards are very relevant to this design problem and this project. During the initial phase of the project, the team spent ample time researching relevant engineering standards to better define the user requirements and engineering specifications. The team consulted both international standards, for instance the ISO and IED standards; as well as standards

local to Bangladesh, like the Bangladesh Standards (BDS). Although many standards were reviewed during the course of this project, the following standards were directly applied to the project:

- IEC 60335-1:2010 Household and Similar Electric Appliances Safety Part 1: General requirements [49]: This International Standard addresses the requirements for safety of electrical appliances for household use, which will be met by our thermoelectric cooling unit. For instance, the standard requires a “rated voltage being not more than 250 V for single-phase appliances”[49], which we have taken into consideration during the development of the device’s electrical system, as well as when estimating the device’s power consumption.
- IEC 60335-2-80:2015 Household and Similar Electrical Appliances - Safety - Part 2-80: Particular Requirements for Fans [50]. This standard addresses common hazards and safety requirements for household and similar electrical appliances that contain fans. We are concerned with this standard, as our solution incorporates two fans. In complying with the safety requirement, we have decided to use “grills” in packaging design to prevent loose parts from flying out at high speed.
- IEC 60529-2004 Degrees of Protection Provided by Enclosures (IP Code): [17] This standard describes a method “to classify the degrees of protection provided by enclosures of electrical equipment for two conditions: (1) the protection of persons against access to hazardous parts and protection of equipment against the ingress of solid foreign objects and (2) the ingress of water.”[17] Since the solution will be used in an area where flooding and extreme humidity is common, the solution must not stop functioning or create hazards when exposed to water. Additionally, the solution incorporates fans that are susceptible to failures due to dust ingress. To avoid failure due to water and dust ingress, it was determined that the system needs to meet an IP-52 rating. This rating is further specified in the engineering standard and was a key element of the durability requirement for the design solution. While developing the final solution, we made specific design decisions to meet this requirement. For example, the electronics are mounted in a waterproof housing which is placed inside a compartment at top of the assembly, as seen in Figure 22 (pg.21). However, design iteration and validation testing are necessary to ensure that the IP-52 rating is met.

We also plan to contact Spreeha to determine if there are additional relevant local standards that we have not addressed.

Conclusion

This project was aimed at developing a solution to provide thermal comfort to urban slum residents in Bangladesh. The project was sponsored by Spreeha, an NGO that provides healthcare, resources and training to underprivileged areas within Bangladesh. Various information sources were explored, as summarized in Table 2 (pg. 4). Information from stakeholder interviews, academic literature, and standards were used to generate user requirements and engineering specifications, as summarized in Table 3 (pg. 6).

Concept generation techniques including individual brainstorming and functional decomposition were used to develop concepts that could decrease temperature, decrease humidity, and increase air speed experienced by urban slum residents in their homes. A morphological chart, shown in Table 4 (pg. 13), was created to organize these ideas into their appropriate sub-functions. Engineering analysis was conducted to assess the feasibility and cooling capability of direct evaporative cooling, ventilation via thermal chimney, a reflective tarp, thermoelectric cooling, and single fan ventilation. From this, a Pugh

Chart, shown in Table 6 (pg. 17) rated each concept against a baseline solution for how well it met the user requirements.

The final selected concept was thermoelectric cooling supplemented with fan ventilation. Further analysis was conducted, which was the main source of verification due to inability to prototype and test. This analysis verified that the solution meets the cooling requirements. Design adjustments were made to mitigate risks of safety issues (such as burning, exposed electrical components, and sharp parts), cross contamination of hot and cold airflows which could decrease cooling power, and condensation buildup. The final CAD design is shown in Figures 22-23 (pg.21). A detailed engineering analysis is outlined on pages 22-34. The final estimated cost of the solution is \$43.34, which is within the target cost. The process for verifying the design's ability to meet user requirements and engineering specifications was outlined in the flowchart shown in Figure 33 (pgs. 35-37).

Strengths of this design include its ability to cool without adding humidity to the system. A CFD simulation verified the Matlab model as accurate, which predicts the solution's cooling ability. In addition, the final design is small, easy to transport, requires non-invasive installation, and does not require resources other than electricity to function. This design could be improved by decreasing its power consumption and decreasing manufacturing costs. This solution is limited in its ability to cool a large space, as it is most effective in providing cooling comfort to a user close to the cold air outlet. Furthermore, it is essential that the hot air stream is properly expelled from the living space.

During this design process, the Engineering Code of Ethics was closely followed. Designing for sustainability was also very important, especially since the cooling solution is to be deployed in a low-resource area. Existing engineering standards were used as metrics for determining engineering specifications and user requirements, and also referenced when evaluating the final design.

Next steps for the project include user validation in Bangladesh when it becomes safe to do so. This project will be passed on to future BLUElab members and discussed with Spreeha in hopes of implementing it in the future.

Information Sources and References

- [1] "Spreeha." Spreeha Foundation. Accessed April 19, 2020. <http://www.Spreeha.org/>.
- [2] "Bangladesh Climate Data Portal." Bangladesh Climate Data. Accessed April 19, 2020. <http://bmd.wowspace.org/team/homex.php>.
- [3] "Climate & Weather Averages in Dhaka, Bangladesh." timeanddate.com. Accessed April 19, 2020. <https://www.timeanddate.com/weather/bangladesh/dhaka/climate>.
- [4] Mallick, Fuad H. "Thermal Comfort and Building Design in the Tropical Climates." *Energy and Buildings* 23, no. 3 (1996): 161–67.
- [5] Iqbal, A. (Photo Album). (2019). *BLUELabs Bangladesh 2019* [album]. Dhaka, Bangladesh
- [6] Appendix Table 3. "Density, Specific Heat Capacity and Thermal Conductivity of Common Metallic Materials." Accessed April 19, 2020.
- [7] Bergman, T. L., Adrienne Lavine, and Frank P. Incropera. *Fundamentals of Heat and Mass Transfer*. Hoboken, NJ: John Wiley & Sons, Inc., 2019. p. 989.
- [8] Iqbal, Abrar. Personal Interview. 21 January 2020.
- [9] Hossain, Abdullah. "Rayerbazar Slum Upgrading." LinkedIn SlideShare, October 17, 2017. https://www.slideshare.net/ANTHOHEEN/rayerbazar-slum-upgrading?from_action=save.
- [10] Butcher, Ken J. "Air Conditioning , Heating, Ventilating And Refrigeration." *Mechanical Design*, 1967, 8–9.
- [11] ISO 5149-1: 2014. "Refrigerating systems and heat pumps — Safety and environmental Requirements" Part 1: Definitions, classification and selection criteria. ISO.
- [12] "American Society Of Heating, Refrigeration And Air-Conditioning Engineers, Ashrae, Inc." *A-To-Z Guide to Thermodynamics, Heat and Mass Transfer, and Fluids Engineering*, n.d.
- [13] Seva, Rosemary R., Katherine Grace T. Gosiaco, Ma. Crea Eurice D. Santos, and Denise Mae L. Pangilinan. "Product Design Enhancement Using Apparent Usability and Affective Quality." *Applied Ergonomics* 42, no. 3 (March 2011): 511–17. <https://doi.org/10.1016/j.apergo.2010.09.009>.
- [14] Poland, Kristin M. "The Ergonomics and Biomechanics of an Awkward Barrel Lift." 1998.
- [15] Ahmed, Rafique. "National Encyclopedia of Bangladesh-Climate." Banglapedia, 1998. <http://en.banglapedia.org/index.php?title=Climate>.
- [16] Merkel, Alexander. "Dhaka Climate Summary." Climate-Data.Org, <https://en.climate-data.org/asia/bangladesh/dhaka-division/dhaka-1062098/#climate-graph>.
- [17] International Electrotechnical Commission. IEC 60529. *Degrees of protection provided by enclosures (IP Code)*. International standard. 2013. p. 21. ISBN 9782832210864. OCLC 864643678.
- [18] ASHRAE. *ASHRAE Design Guide for Dedicated Outdoor Air Systems*. ASHRAE Publications / American Society of Heating, Refrigerating and Air-Conditioning Engineers, 2017.
- [19] Chun-Che Huang, and A. Kusiak. "Modularity in Design of Products and Systems." *IEEE Transactions on Systems, Man, and Cybernetics - Part A: Systems and Humans*, vol. 28, no. 1, Jan. 1998, pp. 66–77. DOI.org (Crossref), doi:10.1109/3468.650323.
- [20] Center for Socially Engaged Design. (2017). "Concept Development Tools - Functional Decomposition"
- [21] Onyanga-Omara, J. (2013, September 14). Plastic bag backlash gains momentum. Retrieved from <https://www.bbc.com/news/uk-24090603>
- [22] Harris, P Stephen, and Roger A LaBoube. "Understanding the Engineering Safety Factor in Building Design," n.d., 3.
- [23] e>Electronics>Home Appliances>Fan. "Othoba.Com," n.d. <https://www.othoba.com/fan>.
- [24] "Friedrich Air Conditioning Company- Room Air Conditioners Limited Warranty," n.d. https://content.abt.com/documents/77904/SL24N30C_warranty.pdf.
- [25] "Module 10: Absorption Refrigeration." CIBSE Journal. Accessed February 26, 2020. <https://www.cibsejournal.com/cpd/modules/2009-11/>.
- [26] "D.I.Y. Inspired Evaporative Cooler Design for Remote Military Applications: Evaporative Cooler, Cooler Designs, Cool Stuff." Pinterest. Accessed February 26, 2020.

- [https://www.pinterest.com/pin/562738915917140522/.](https://www.pinterest.com/pin/562738915917140522/)
- [27] “Reflective Mylar Film.” GreenhouseBay.com. Accessed February 26, 2020. <https://greenhousebay.com/product/reflective-mylar-film/>.
- [28] Crotti, Nancy. “Thermoelectric Cooler Solutions for Medical Applications.” Medical Design and Outsourcing, November 22, 2019. <https://www.medicaldesignandoutsourcing.com/thermoelectric-cooler-solutions-for-medical-applications/>.
- [29] “Drierite Indicating Desiccant 8 Mesh, 5lb Jar.” Certified Material Testing Products. Accessed February 26, 2020. <https://www.certifiedmtp.com/drierite-indicating-desiccant-8-mesh-5lb-jar/>.
- [30] “Silica Gel Packet.” indiamart.com. Accessed February 26, 2020. <https://www.indiamart.com/proddetail/silica-gel-packet-5034403373.html>.
- [31] “How Does a Dehumidifier Work?” Achoo! Blog. Accessed February 26, 2020. <https://www.achooallergy.com/blog/learning/how-does-a-dehumidifier-work/>.
- [32] “Top 5 Natural Dehumidifier Plants for High Humid Homes.” Home Products HQ, 16 Feb. 2020, homeproductshq.com/natural-dehumidifier-plants/.
- [33] “Solar/Thermal Chimney.” Home. Accessed February 26, 2020. <http://ae390systemsvariety-group6.weebly.com/solarthermal-chimney.html>.
- [34] Stand-alone Fan: Spreeha. Personal Interview. 24 February 2020.
- [35] Gerhart, Philip M., et al. Munson, Young, and Okiishi. “Fundamentals of Fluid Mechanics.” Wiley, 2019.
- [36] Kaviany, M. “Heat Transfer Physics”. Cambridge University Press, 2014.
- [37] Monteith, J.L., and Unsworth, M.H. 2008. “Principles of Environmental Physics”. Third Ed. AP, Amsterdam. <http://store.elsevier.com/Principles-of-Environmental-Physics/John-Monteith/isbn-9780080924793/>
- [38] Mun, Kwak, Kim, and Huh. “A Comprehensive Thermal Comfort Analysis of the Cooling Effect of the Stand Fan Using Questionnaires and a Thermal Manikin.” Sustainability 11, no. 18 (September 17, 2019): 5091. <https://doi.org/10.3390/su11185091>.
- [39] He, Yingdong, Nianping Li, Xiang Wang, Meiling He, and De He. “Comfort, Energy Efficiency and Adoption of Personal Cooling Systems in Warm Environments: A Field Experimental Study.” International Journal of Environmental Research and Public Health 14, no. 11 (November 17, 2017): 1408. <https://doi.org/10.3390/ijerph14111408>.
- [40] Berkeley.edu. “CBE Thermal Comfort Tool,” n.d. <https://comfort.cbe.berkeley.edu/>.
- [41] “BXQINLENX TEC1-12710 Thermoelectric Cooler Peltier 40X40.” Amazon.com. Accessed April 19, 2020. <https://www.amazon.com/BXQINLENX-TEC1-12710-Thermoelectric-Cooler-Peltier/dp/B011KFI29Y>.
- [42] ‘Nxtop Aluminum Heatsink Heatsink Module Cooler Fin for High Power Led Amplifier Transistor Semiconductor Devices with 100mm (L) x 69mm(W) x 36mm(H).’ Amazon.com. Accessed April 19, 2020. <https://www.amazon.com/Nxtop-Aluminum-Amplifier-Transistor-Semiconductor/dp/B07DH5T2RW/>
- [43] “Aluminum Heat Radiator Heatsink Cooling Fin 150x69x37mm Silver Tone.” Amazon.com. Accessed April 19, 2020. <https://www.amazon.com/dp/B00VG6WPKK/>
- [44] “MakerFocus 4pcs 3D Printer Fan 12V, 40mm 12 Volt Fan 0.08A DC.” Amazon.com. Accessed April 19, 2020. <https://www.amazon.com/MakerFocus-Printer-40X40X10mm-Appliances-Replacement/dp/B07CH6YC32/>
- [45] “Gdstime 80mm x 80mm x 10mm DC 5V 0.25A Brushless Cooling Fan.” Amazon.com. Accessed April 19, 2020. <https://www.amazon.com/dp/B00N1Y4RLU/>
- [46] “80 mm PC CPU Case Fans DC 12V Computer Fan 80mm.” Amazon.com. Accessed April 19, 2020. <https://www.amazon.com/Computer-Performance-Cooling-Supply-3000RPM/dp/B07R52RY3P/>

- [47] "GDSTIME 4500RPM 8cm 80mm x 80mm x 25mm 12v Big Airflow High Speed Dual Ball Bearing Brushless DC Cooling Fan." Amazon.com. <http://amazon.com/dp/B00N1Y3R2K/>
- [48] "DAOKI 2PCS TEC1-12706 12V 60W Heatsink Thermoelectric Cooler Cooling Peltier Plate Module 12V 6A." Amazon.com. Accessed April 19, 2020. <https://www.amazon.com/DAOKI-TEC1-12706-Heatsink-Thermoelectric-Cooling/dp/B00XT0OZY0/>
- [49] International Electrotechnical Commission. *Household and Similar Electrical Appliances - Safety - Part 1: General Requirements*. IEC 60335-1:2010.
- [50] International Electrotechnical Commission. *Household and Similar Electrical Appliances - Safety - Part 2-80: Particular Requirements for Fans*. IEC 60335-2-80:2015.

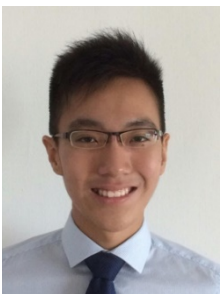
Author Bios

Rahul Saxena



Rahul is a senior from Troy, MI. He decided to study mechanical engineering to solve important problems while engaging his desire to build and create. He was heavily involved in the FIRST robotics program throughout his childhood. He enjoys hands-on projects and is interested in the field of dynamics and controls. He plans on pursuing a master's degree in mechanical engineering after graduation. He also enjoys exercising, listening to new music, and watching U of M sports.

Derek Tan



Derek is a senior from Singapore. He is interested in Mechanical Engineering because he was inspired by his mother and older brother who are chemical and mechanical engineers respectively. When he was little, he particularly enjoyed building zoids (a mechanically actuated robot assembly set) and playing with Lego. When he was older, he was tasked by his parents to repair common household appliances. He also loves tinkering with mechatronics systems. After graduation, he will be working for the autonomous robotics engineering firm back in Singapore. In his free time, he enjoys practicing martial arts (Thai kickboxing) and game development in Unity platform. He aspires to set up a social enterprise with the goal of providing rehabilitation to the disabled through games, technology or engineering in general.

Maddy Trevisan



Maddy is fourth year senior from Farmington, MI. She decided to study mechanical engineering as a way to develop technical and problem solving skills that can be used to improve the quality of life of others. She is very interested in medical device design and will be pursuing a Masters of Design Science degree at U of M following graduation. Maddy is also an athlete on the cross country and track team at the University of Michigan, where she specializes in the long distance events. She enjoys watching sports, being outside, and spending time with family and friends.

Mihir Upadhye



Mihir is a senior from Okemos, MI. His interest in engineering began in high school where he participated in stage crew, building sets for the school's theatrical productions. Upon arriving to the University of Michigan, his growing interest in the automotive industry brought him to select mechanical engineering for his major. After graduation, he plans to pursue an accelerated master's program at UofM to better his knowledge of materials engineering for use in the automotive or aerospace industries. In his free time, he enjoys building speakers, finding new music, and going on road trips.

Betty Wan



Betty is a fourth-year senior from Beijing, China. She decided to study mechanical engineering because she likes hands-on activities, and the broadness in ME allows her to explore the various fields within the subject. After graduation, she plans to pursue a master's degree in ME to further build up her knowledge in robotics. In her free time, she enjoys doing photography, dancing, and trying out new foods.

Appendix A: Tables A.1-A.2, Figure A.1

Table A.1: Matlab results of key parameters for Configuration 4.

| Variables | Representation | Optimal Current | Higher COP |
|-----------------------------------|--|-----------------|--------------|
| Input Current [A] | J_e | 8.9 | 4.8 |
| Power Required [W] | P_{in} | 135.1 | 38.5 |
| Inlet Air Temperature [K] | $(T_{\infty,C})_{in}, (T_{\infty,H})_{in}$ | 308.2 | 308.2 |
| Cold Mass Flow Rate [CFM] | \dot{m}_c | 16.5 | 16.5 |
| Cold Air Speed [m/s] | $(U_{\infty})_c$ | 2.2 | 2.2 |
| Chip Temperature – Cold [K] | T_c | 297.4 | 299.6 |
| Cooling Power [W] | Q_c | 58.2 | 46.1 |
| Outlet Air Temperature - Cold [K] | $(T_{\infty,C})_{out}$ | 301.8 | 303.1 |
| Temperature Drop – Cold [K] | $(\Delta T)_c$ | 6.4 | 5.1 |
| Hot Mass Flow Rate [CFM] | \dot{m}_H | 59.0 | 59.0 |
| Hot Air Speed [m/s] | $(U_{\infty})_H$ | 7.4 | 7.4 |
| Chip Temperature – Hot [K] | T_H | 338.9 | 321.6 |
| Heating Power [W] | Q_H | 193.3 | 84.5 |
| Outlet Air Temperature - Hot [K] | $(T_{\infty,H})_{out}$ | 316.3 | 311.7 |
| Coefficient of Performance [%] | COP | 43.1 | 119.7 |

Table A.2: Parameters characterizing two thermoelectric chips: TEC1-12706 and TEC1-12710.

| Variables | TEC1-12706 [48] | TEC1-12710 [41] |
|---|------------------|-------------------|
| $\alpha_{s(p \text{ or } n)} [\mu V/K]$ | 2.3e-04, -2.1e-0 | 2.3e-04, -2.1e-04 |
| $\rho_{e(p \text{ or } n)} [Kg/m^3]$ | 1e-05, 1e-05 | 1e-05, 1e-05 |
| $K_{(p \text{ or } n)} [W/mK]$ | 1.70, 1.45 | 1.70, 1.45 |
| N_{TE} [pairs] | 110 | 126 |
| L [m] | 0.0022 | 0.0019 |
| $A_k [m^2]$ | 1.21e-06 | 1.82e-06 |
| $R_{k,H-C} [W/mK]$ | 2.0661 | 1.235 |
| $R_{e,H-C} [W/mK]$ | 0.0102 | 0.0058 |

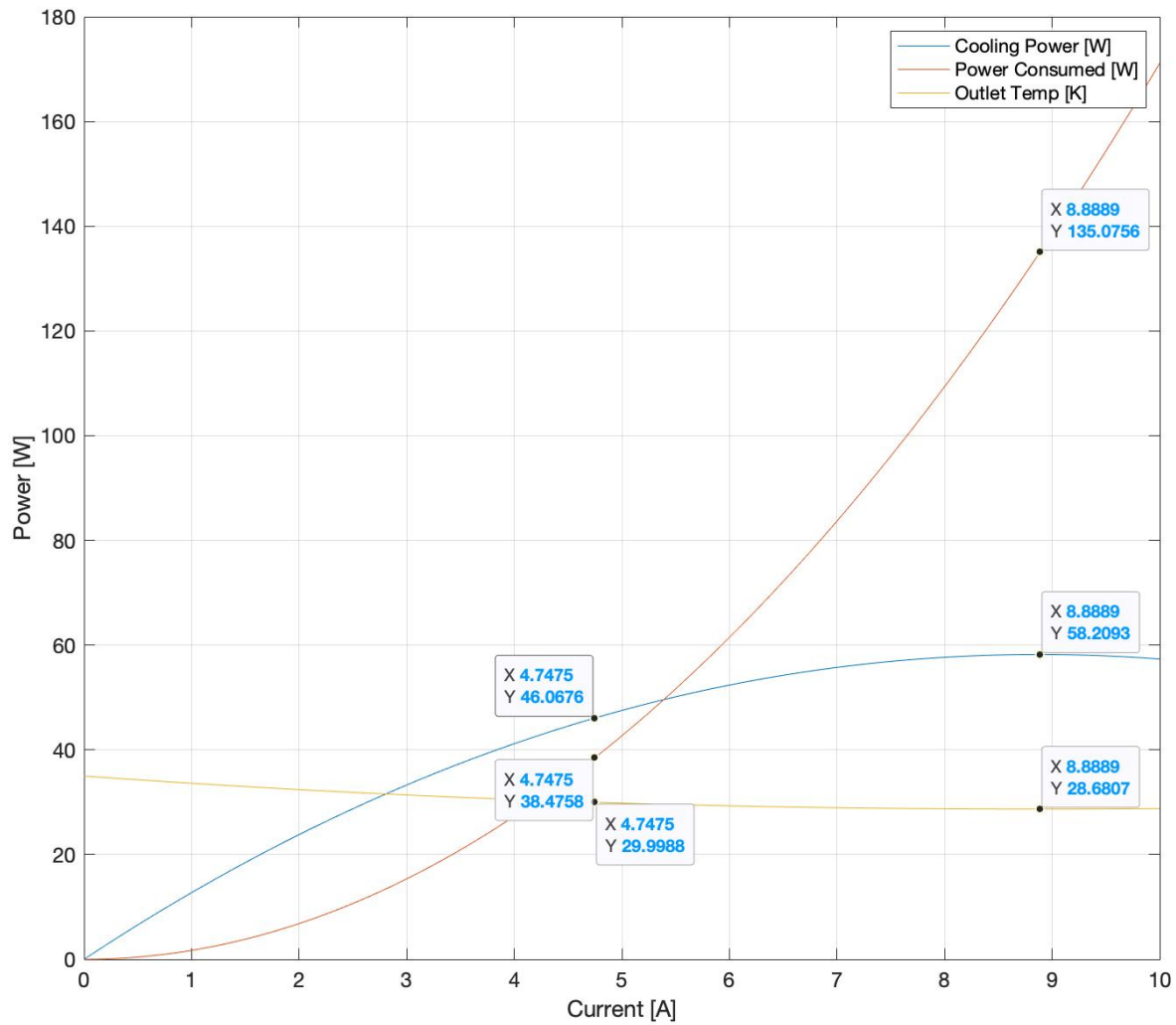


Figure A.1: Cooling power against current through the abovementioned thermoelectric Configuration 4

Appendix B: Full-Sized Pugh Chart, Table B.1

Table B.1: A larger view of the Pugh chart used for concept selection.

| | | | | 1 | 2 | 3 | 4 | 5 | 6 | 7 | 8 | 9 | 10 |
|--|---------------------------|--------------------------|---------------|-------|------------|--------------------------|--------------------------------|-----------------|------------------|---------|----------|-----------------------------|-------------|
| | | | Requirement | Safe | Affordable | Adequate Cooling Ability | Compatibility with House Types | Easily Operated | Easily Installed | Durable | Reliable | Easily Repaired or Replaced | Sustainable |
| Plausible Concept Combinations | | | WEIGHT (1-10) | 10 | 10 | 10 | 7 | 7 | 7 | 7 | 8 | 6 | 4 |
| Temperature | Humidity | Air Speed | TOTAL SCORE | Score | Score | Score | Score | Score | Score | Score | Score | Score | Score |
| Vapor Compression Refrigeration Cycle | - | Fan | 0 | 0 | 0 | 0 | 0 | 0 | 0 | 0 | 0 | 0 | 0 |
| Absorption Refrigeration Cycle | - | Fan | -30 | 0 | -1 | -1 | 0 | 0 | -1 | -1 | -1 | 0 | 3 |
| Direct Evaporative Cooling | Desiccant Dehumidifaction | Fan | 25 | -2 | 1 | -1 | 1 | -2 | 2 | 2 | 2 | 2 | -1 |
| Direct Evaporative Cooling | Desiccant Dehumidifaction | Ceiling Fan Modification | -5 | -2 | 2 | -2 | 2 | -2 | -2 | 1 | 2 | 1 | 0 |
| Direct Evaporative Cooling | - | Fan | 66 | 0 | 3 | -1 | 0 | -2 | 2 | 2 | 2 | 2 | 1 |
| Indirect Evaporative Cooling | - | Fan | 53 | 1 | 0 | -1 | 0 | -1 | 2 | 2 | 2 | 2 | 1 |
| Indirect Evaporative Cooling | - | Ceiling Fan Modification | 10 | -1 | 1 | -2 | 2 | -1 | -2 | 1 | 2 | 1 | 2 |
| Thermoelectric Cooling | - | Fan | 84 | 1 | 1 | -1 | 2 | 1 | 1 | 2 | 2 | 2 | 1 |
| Thermal Chimney | - | Fan | 20 | 1 | 2 | -1 | -2 | 1 | -2 | 1 | 1 | 1 | 0 |
| - | - | Portable Handheld Fan | 58 | 0 | 3 | -3 | 3 | 2 | 3 | 0 | 0 | 1 | -1 |
| High Reflectivity, Low Absorptivity Tarp | - | - | 52 | 3 | 0 | -2 | -1 | 3 | -2 | 0 | 3 | 3 | 0 |
| - | - | Thermal Chimney | 38 | 1 | 2 | -2 | -2 | 3 | -2 | 1 | 2 | 2 | 0 |
| - | Indoor Plants | - | -39 | 3 | 3 | -3 | 0 | -2 | -1 | -2 | -3 | -3 | 2 |

Appendix C: Exploded CAD of Final Product

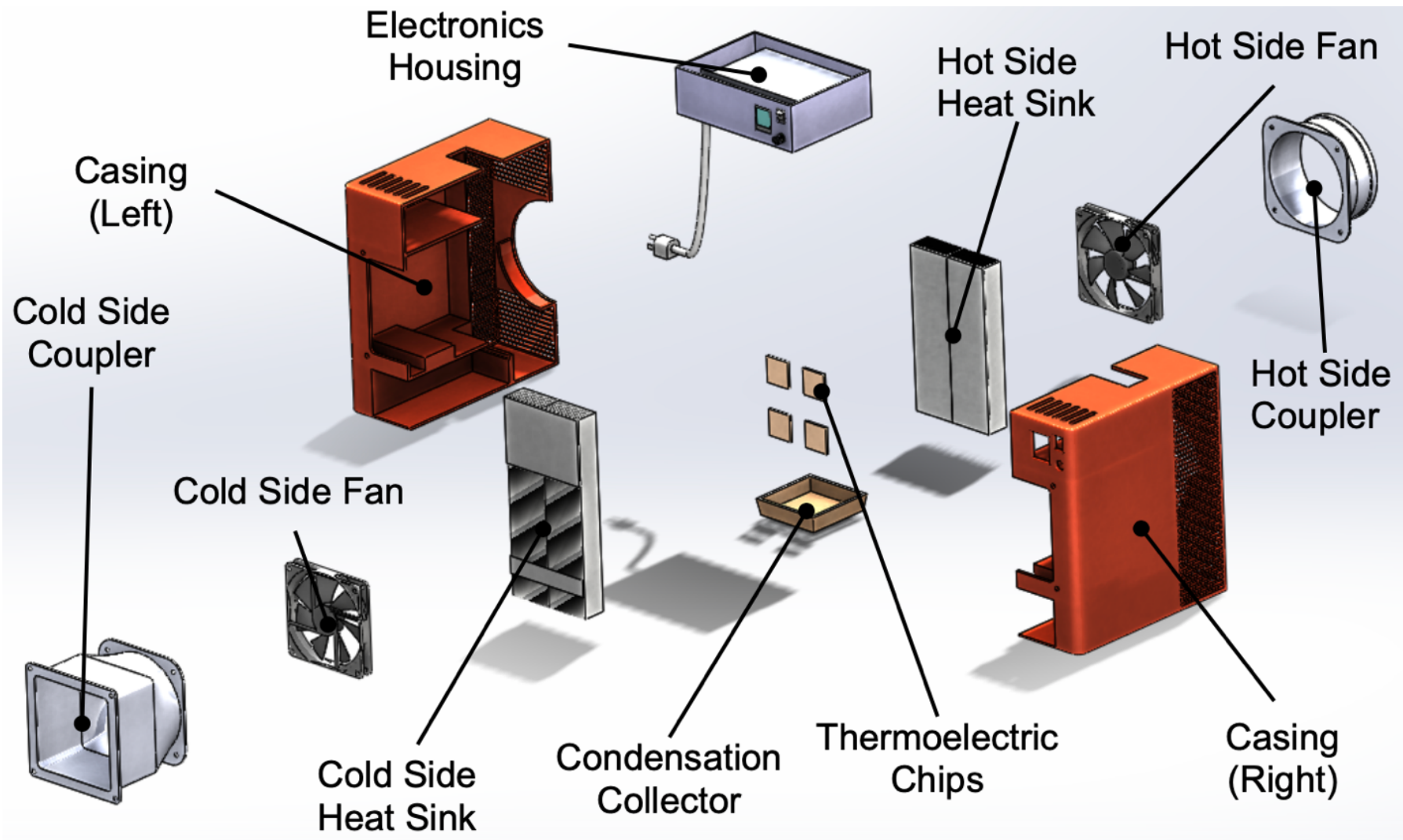


Figure C.1: CAD of final product broken down in exploded view on Solidworks.

Appendix D: Bill of Materials for the Final Design Solution

Table D.1: The Bill of Materials for the final design solution.

| Thermoelectric Cooler Bill of Materials | | | | | | |
|---|-----------------------------------|---|--|--------|-----------------------------|---|
| Peltier System | TEC1-12710 | 4 | 9-12V input (Depending on power supply) | \$1.30 | ALIBABA | https://www.alibaba.com/ Peltier Cooling Element |
| | Cold Side CPU Fan (14cm x 14cm) | 1 | 5.5-13.8V, 0.18A input, 2200 RPM, 120 CFM | \$2.95 | ALIBABA | https://www.alibaba.com/ To Cool hot side fins (Reduce T_h) |
| | Hot Side CPU Fan (14cm x 14cm) | 1 | 5.5-13.8V, 0.35A input, 3000 RPM, 143 CFM | \$2.95 | ALIBABA | https://www.alibaba.com/ To blow air into cold fins to be cooled |
| | Hot Side Fin (250x69x37mm) | 2 | 69x37mm, cut to length. \$2.5/kg (each kg can make 2) | \$1.25 | ALIBABA | https://www.alibaba.com/ Increase surface area to absorb heat from cold side air |
| | Cold Side Fin (300x69x37mm) | 4 | 150x69x37mm AL 6063 Heatsink, 4 in total | \$0.50 | ALIBABA | https://www.alibaba.com/ Longer fin to increase cooling + more peltier elements |
| | Thermal Paste (4g) | 1 | 8.5 W/mK, 4g | \$1.10 | ALIBABA | https://www.alibaba.com/ Minimize contact resistance between peltier element and sink |
| | Thermal Insulation | 1 | 3mm thick, -40 to 150 F° | \$0.04 | ALIBABA | https://hunrade.en.alibaba.com/ Minimize heat transfer between hot and cold side fins |
| Ducts | Hot Coupler | 1 | 15mm duct (Inner Radius) | \$1.96 | Injection Molding (N=10000) | 3D Hub online quote Connect fan to conduit pipe |
| | Hot Side Vent Hose | 1 | 15mm Duct (Inner Radius), per meter | \$0.27 | ALIBABA | https://www.alibaba.com/ Channel hot air out of room through window/door |
| | Cold Coupler | 1 | 15mm duct (Inner Radius) - CAN CHANGE | \$3.85 | Injection Molding (N=10000) | 3D Hub online quote Connect fins to outlet fan |
| Electronics | AC to DC Unit (12V - 20A) | 1 | Dimensions: 20mm x 11mm x 5mm | \$3.00 | ALIBABA | https://www.alibaba.com/ Connect to AC-DC 5V unit in parallel to mains to power fan |
| | On-off Switch | 1 | Mini Switch 2 PIN, 10x15mm | \$0.10 | ALIBABA | https://www.alibaba.com/ On-off switch |
| | Thermocouples with display | 2 | Electronic digital display thermometer with waterproof probe | \$0.50 | ALIBABA | https://www.alibaba.com/ Measure air temp of outlet air stream |
| | DC Motor Voltage Controller - 12V | 1 | Control motor speed of fan with potentiometer - 2 pieces | \$1.47 | ALIBABA | https://www.alibaba.com/ Controller to control speed of cold side fan |
| Packaging | Power Mains Chord for DC Unit | 1 | 3A 5A 10A 13A 110V | \$0.50 | ALIBABA | https://www.alibaba.com/ Supply power for DC unit which power Peltier unit |
| | Casing, LHS | 1 | ABS, normal finish, black | \$5.38 | Injection Molding (N=10000) | https://zdcpcu.en.alibaba.com/ The LHS of the package |
| | Casing, RHS | 1 | ABS, normal finish, black | \$5.38 | Injection Molding (N=10000) | https://zdcpcu.en.alibaba.com/ Symmetrical with the LHS, thus N=20000 |
| | Electronics housing | 1 | ABS, normal finish, black | \$3.59 | Injection Molding (N=10000) | 3D Hub online quote Houses and secures electronics components and wirings |
| Condensor Bowl | | 1 | ABS, normal finish, black | \$0.10 | ALIBABA | https://www.alibaba.com/ To condense water dripped from the cold side |
| Total | | | \$43.34 | | | |

Acknowledgements

This project was made possible with the help of peers, subject matter experts, and faculty members at the University of Michigan. We would first like to thank Abrar Iqbal and Kiersten White, two University of Michigan peers involved in BLUELab, for providing the necessary background information and context for this project. Joanna Millunchick, the ME librarian at U of M, provided resources and guidance for conducting research during the early stages of design. We would also like to acknowledge Professor Kathleen Sienko, who offered guidance and resources for designing for low resource settings. Grace Burleson and Caroline Soyars, both who work closely with the university's Center for Socially Engaged Design, gave us insight into concept generation and cost benchmarking. John Laidlaw, who manages the ME X50 test labs, was helpful in providing testing equipment for empirical testing (before we were limited by COVID-19 restrictions). We are very appreciative of all the help Julio Ferreira, PhD candidate, has provided in conducting the CFD analysis. Last but not least, we want to thank our faculty advisor, Professor Massoud Kaviany, for his guidance and support for this project from start to finish. His expertise in heat transfer analysis, positive encouragement, and feedback was crucial to this design experience, and we owe our success to him.